

INTERNATIONAL  
STANDARD

IEC  
61000-4-33

First edition  
2005-09

BASIC EMC PUBLICATION

---

---

**Electromagnetic compatibility (EMC) –  
Part 4-33:  
Testing and measurement techniques –  
Measurement methods for high-power  
transient parameters**

IECNORM.COM : Click to view the full PDF of IEC 61000-4-33:2005



Reference number  
IEC 61000-4-33:2005(E)

## Publication numbering

As from 1 January 1997 all IEC publications are issued with a designation in the 60000 series. For example, IEC 34-1 is now referred to as IEC 60034-1.

## Consolidated editions

The IEC is now publishing consolidated versions of its publications. For example, edition numbers 1.0, 1.1 and 1.2 refer, respectively, to the base publication, the base publication incorporating amendment 1 and the base publication incorporating amendments 1 and 2.

## Further information on IEC publications

The technical content of IEC publications is kept under constant review by the IEC, thus ensuring that the content reflects current technology. Information relating to this publication, including its validity, is available in the IEC Catalogue of publications (see below) in addition to new editions, amendments and corrigenda. Information on the subjects under consideration and work in progress undertaken by the technical committee which has prepared this publication, as well as the list of publications issued, is also available from the following:

- **IEC Web Site ([www.iec.ch](http://www.iec.ch))**
- **Catalogue of IEC publications**

The on-line catalogue on the IEC web site ([www.iec.ch/searchpub](http://www.iec.ch/searchpub)) enables you to search by a variety of criteria including text searches, technical committees and date of publication. On-line information is also available on recently issued publications, withdrawn and replaced publications, as well as corrigenda.

- **IEC Just Published**

This summary of recently issued publications ([www.iec.ch/online\\_news/\\_justpub](http://www.iec.ch/online_news/_justpub)) is also available by email. Please contact the Customer Service Centre (see below) for further information.

- **Customer Service Centre**

If you have any questions regarding this publication or need further assistance, please contact the Customer Service Centre:

Email: [custserv@iec.ch](mailto:custserv@iec.ch)  
Tel: +41 22 919 02 11  
Fax: +41 22 919 03 00

# INTERNATIONAL STANDARD

IEC  
**61000-4-33**

First edition  
2005-09

BASIC EMC PUBLICATION

---

---

**Electromagnetic compatibility (EMC) –  
Part 4-33:  
Testing and measurement techniques –  
Measurement methods for high-power  
transient parameters**

IECNORM.COM : Click to view the full PDF of IEC 61000-4-33:2005

© IEC 2005 — Copyright - all rights reserved

No part of this publication may be reproduced or utilized in any form or by any means, electronic or mechanical, including photocopying and microfilm, without permission in writing from the publisher.

International Electrotechnical Commission, 3, rue de Varembé, PO Box 131, CH-1211 Geneva 20, Switzerland  
Telephone: +41 22 919 02 11 Telefax: +41 22 919 03 00 E-mail: [inmail@iec.ch](mailto:inmail@iec.ch) Web: [www.iec.ch](http://www.iec.ch)

---

---



Commission Electrotechnique Internationale  
International Electrotechnical Commission  
Международная Электротехническая Комиссия

PRICE CODE

**XB**

*For price, see current catalogue*

## CONTENTS

FOREWORD .....	4
INTRODUCTION .....	6
1 Scope .....	7
2 Normative references .....	7
3 Terms and definitions .....	8
4 Measurement of high-power transient responses .....	9
4.1 Overall measurement concepts and requirements .....	9
4.2 Representation of a measured response .....	12
4.3 Measurement equipment .....	12
4.4 Measurement procedures .....	27
5 Measurement of low frequency responses .....	27
6 Calibration procedures .....	28
6.1 Calibration of the entire measurement channel .....	28
6.2 Calibration of individual measurement channel components .....	31
6.3 Approximate calibration techniques .....	37
Annex A (normative) Methods of characterizing measured responses .....	40
Annex B (informative) Characteristics of measurement sensors .....	45
Annex C (normative) HPEM measurement procedures .....	59
Annex D (informative) Two-port representations of measurement chain components .....	62
Bibliography .....	69
Figure 1 – Illustration of a typical instrumentation chain for measuring high-power transient responses .....	10
Figure 2 – Illustration of a balanced sensor and cable connecting to an unbalanced (coaxial) line where $I_{\text{out}} + I_{\text{in}} = I_1$ .....	16
Figure 3 – Examples of some simple baluns [4b] .....	18
Figure 4 – A typical circuit for an in-line attenuator in the measurement chain .....	18
Figure 5 – Illustration of the typical attenuation of a nominal 20 dB attenuator for a 50- $\Omega$ system, as a function of frequency .....	19
Figure 6 – Typical circuit diagram for an in-line integrator .....	20
Figure 7 – Plot of the transfer function of the integrating circuit of Figure 6 .....	20
Figure 8 – Illustration of the frequency dependent per-unit-length signal transmission of a standard coaxial cable, and a semi-rigid coaxial line .....	21
Figure 9 – Illustration of sensor cable routing in regions not containing EM fields .....	24
Figure 10 – Treatment of sensor cables when located in a region containing EM fields .....	25
Figure 11 – Conforming cables to local system shielding topology .....	26
Figure 12 – Correct and incorrect methods of cable routing .....	27
Figure 13 – The double-ended TEM Cell for providing a uniform field illumination for probe calibration .....	29
Figure 14 – Illustration of the single-ended TEM cell and associated equipment .....	30
Figure 15 – Dimensions of a small test fixture for probe calibration .....	30

Figure 16 – Electrical representation of a measurement chain, (a) with the E-field sensor represented by a general Thevenin circuit, and (b) the Norton equivalent circuit for the same sensor.....	31
Figure 17 – Example of a simple E-field probe.....	34
Figure 18 – Plot of the real and imaginary parts of the input impedance, $Z_i$ , for the E-field sensor of Figure 17.....	34
Figure 19 – Plot of the magnitude of the short-circuit current flowing in the sensor input for different angles of incidence, as computed by an antenna analysis code .....	35
Figure 20 – Plot of the magnitude of the effective height of the sensor for different angles of incidence.....	36
Figure 21 – High frequency equivalent circuit of an attenuator element .....	39
Figure A.1 – Illustration of various parameters used to characterize the pulse component of a transient response waveform $R(t)$ .....	41
Figure A.2 – Illustration of an oscillatory waveform frequently encountered in high-power transient EM measurements.....	41
Figure A.3 – Example of the calculated spectral magnitude of the waveform of Figure A.2 ..	44
Figure B.1 – Illustration of a simple E-field sensor, together with its Norton equivalent circuit.....	46
Figure B.2 – Magnitude and phase of the normalized frequency function $\tilde{F}(\omega\tau)$ for the field sensor .....	47
Figure B.3 – Illustration of a simple B-field sensor, together with its Thevenin equivalent circuit .....	49
Figure B.4 – Illustration of an E-field sensor over a ground plane used for measuring the vertical electric field, or equivalently, the surface charge density.....	50
Figure B.5 – Illustration of the half-loop B-dot sensor used for measuring the tangential magnetic field, or equivalently, the surface current density .....	52
Figure B.6 – Simplified concept for measuring wire currents .....	53
Figure B.7 – Construction details of a current sensor .....	54
Figure B.8 – Example of the measured sensor impedance magnitude of a nominal $1 \Omega$ current sensor.....	55
Figure B.9 – Geometry of the in-line I-dot current sensor .....	55
Figure B.10 – Design concept for a coaxial cable current sensor .....	56
Figure B.11 – Shape and dimensions of a CIP-10 coaxial cable current sensor.....	57
Figure B.12 – Configuration of a coaxial cable I-dot current sensor.....	57
Figure D.1 – Voltage and current relationships for a general two-port network .....	62
Figure D.2 – Voltage and current definitions for the chain parameters.....	63
Figure D.3 – Cascaded two-port networks.....	64
Figure D.4 – Representation of the of a simple measurement chain using the chain parameter matrices.....	64
Figure D.5 – Simple equivalent circuit for the measurement chain .....	65
Figure D.6 – A simple two-port network modelled by chain parameters .....	65
Table A.1 – Examples of time waveform p-norms.....	42
Table A.2 – Time waveform norms used for high-power transient waveforms .....	42
Table D.1 – Chain parameters for simple circuit elements.....	66

## INTERNATIONAL ELECTROTECHNICAL COMMISSION

## ELECTROMAGNETIC COMPATIBILITY (EMC) -

Part 4-33: Testing and measurement techniques –  
Measurement methods for high-power transient parameters

## FOREWORD

- 1) The International Electrotechnical Commission (IEC) is a worldwide organization for standardization comprising all national electrotechnical committees (IEC National Committees). The object of IEC is to promote international co-operation on all questions concerning standardization in the electrical and electronic fields. To this end and in addition to other activities, IEC publishes International Standards, Technical Specifications, Technical Reports, Publicly Available Specifications (PAS) and Guides (hereafter referred to as "IEC Publication(s)"). Their preparation is entrusted to technical committees; any IEC National Committee interested in the subject dealt with may participate in this preparatory work. International, governmental and non-governmental organizations liaising with the IEC also participate in this preparation. IEC collaborates closely with the International Organization for Standardization (ISO) in accordance with conditions determined by agreement between the two organizations.
- 2) The formal decisions or agreements of IEC on technical matters express, as nearly as possible, an international consensus of opinion on the relevant subjects since each technical committee has representation from all interested IEC National Committees.
- 3) IEC Publications have the form of recommendations for international use and are accepted by IEC National Committees in that sense. While all reasonable efforts are made to ensure that the technical content of IEC Publications is accurate, IEC cannot be held responsible for the way in which they are used or for any misinterpretation by any end user.
- 4) In order to promote international uniformity, IEC National Committees undertake to apply IEC Publications transparently to the maximum extent possible in their national and regional publications. Any divergence between any IEC Publication and the corresponding national or regional publication shall be clearly indicated in the latter.
- 5) IEC provides no marking procedure to indicate its approval and cannot be rendered responsible for any equipment declared to be in conformity with an IEC Publication.
- 6) All users should ensure that they have the latest edition of this publication.
- 7) No liability shall attach to IEC or its directors, employees, servants or agents including individual experts and members of its technical committees and IEC National Committees for any personal injury, property damage or other damage of any nature whatsoever, whether direct or indirect, or for costs (including legal fees) and expenses arising out of the publication, use of, or reliance upon, this IEC Publication or any other IEC Publications.
- 8) Attention is drawn to the Normative references cited in this publication. Use of the referenced publications is indispensable for the correct application of this publication.
- 9) Attention is drawn to the possibility that some of the elements of this IEC Publication may be the subject of patent rights. IEC shall not be held responsible for identifying any or all such patent rights.

International Standard IEC 61000-4-33 has been prepared by subcommittee 77C: High power transient phenomena, of IEC technical committee 77: Electromagnetic compatibility.

It has the status of a basic EMC publication in accordance with IEC Guide 107.

The text of this standard is based on the following documents:

FDIS	Report on voting
77C/156/FDIS	77C/160/RVD

Full information on the voting for the approval of this standard can be found in the report on voting indicated in the above table.

This publication has been drafted in accordance with the ISO/IEC Directives, Part 2.

The committee has decided that the contents of this publication will remain unchanged until the maintenance result date indicated on the IEC web site under "http://webstore.iec.ch" in the data related to the specific publication. At this date, the publication will be

- reconfirmed;
- withdrawn;
- replaced by a revised edition, or
- amended.

A bilingual version of this publication may be issued at a later date.

IECNORM.COM : Click to view the full PDF of IEC 61000-4-33:2005

## INTRODUCTION

IEC 61000 is published in separate parts according to the following structure:

### **Part 1: General**

General considerations (introduction, fundamental principles)  
Definitions, terminology

### **Part 2: Environment**

Description of the environment  
Classification of the environment  
Compatibility levels

### **Part 3: Limits**

Emission limits  
Immunity limits (in so far as they do not fall under the responsibility of the product committees)

### **Part 4: Testing and measurement techniques**

Measurement techniques  
Testing techniques

### **Part 5: Installation and mitigation guidelines**

Installation guidelines  
Mitigation methods and devices

### **Part 6: Generic standards**

### **Part 9: Miscellaneous**

Each part is further subdivided into several parts and published either as International Standards or as technical specifications or technical reports, some of which have already been published as sections. Others will be published with the part number followed by a dash and a second number identifying the subdivision (example: 61000-6-1).

## ELECTROMAGNETIC COMPATIBILITY (EMC) –

### Part 4-33: Testing and measurement techniques – Measurement methods for high-power transient parameters

#### 1 Scope

This part of IEC 61000 provides a basic description of the methods and means (e.g., instrumentation) for measuring responses arising from high-power transient electromagnetic parameters. These responses can include:

- the electric ( $E$ ) and/or magnetic ( $H$ ) fields (e.g., incident fields or incident plus scattered fields within a system under test);
- the current  $I$  (e.g., induced by a transient field or within a system under test);
- the voltage  $V$  (e.g., induced by a transient field or within a system under test);
- the charge  $Q$  induced on a cable or other conductor.

NOTE The charge  $Q$  on the conductor is a fundamental quantity that can be defined at any frequency. The voltage  $V$ , however, is a defined (e.g., secondary) quantity, which is valid only at low frequencies. At high frequencies, the voltage cannot be defined as the line integral of the  $E$ -field, since this integral is path-dependent. Thus, for very fast rising pulses (having a large high-frequency spectral content) the use of the voltage as a measurement observable is not valid. In this case, the charge is the desired quantity to be measured.

These measured quantities are generally complicated time-dependent waveforms, which can be described approximately by several scalar parameters, or “observables”. These parameters include:

- the peak amplitude of the response,
- the waveform rise-time,
- the waveform fall-time (or duration),
- the pulse width, and
- mathematically defined norms obtained from the waveform.

This International Standard provides information on the measurement of these waveforms and on the mathematical determination of the characterizing parameters. It does not provide information on specific level requirements for testing.

#### 2 Normative references

The following referenced documents are indispensable for the application of this document. For dated references, only the edition cited applies. For undated references, the latest edition of the referenced document (including any amendments) applies.

IEC 60050-161, *International Electrotechnical Vocabulary (IEV) – Chapter 161: Electromagnetic compatibility*

IEC 61000-2-9, *Electromagnetic compatibility (EMC) – Part 2: Environment – Section 9: Description of HEMP environment – Radiated disturbance*

IEC 61000-2-10, *Electromagnetic compatibility (EMC) – Part 2-10: Environment – Description of HEMP environment – Conducted disturbance*

IEC 61000-4-20, *Electromagnetic compatibility (EMC) – Part 4-20: Testing and measurement techniques – Emission and immunity testing in transverse electromagnetic (TEM) waveguides*

IEC 61000-4-23, *Electromagnetic compatibility (EMC) – Part 4-23: Testing and measurement techniques – Test methods for protective devices for HPEM and other radiated disturbances*

IEC 61000-4-25, *Electromagnetic compatibility (EMC) – Part 4-25: Testing and measurement techniques – HEMP immunity test methods for equipment and systems*

### 3 Terms and definitions

For the purposes of this part of IEC 61000, the following terms and definitions, together with those in IEC 60050-161 apply.

#### 3.1

##### **electrically small**

refers to the size of an object relative to the wavelength of the electromagnetic field. When the object is much smaller than the wavelength, it is said to be electrically small

#### 3.2

##### **equivalent area**

an intrinsic parameter of a magnetic flux sensor (loop) that relates the open circuit voltage of the sensor to the time rate of change of the magnetic flux density linking the sensor

#### 3.3

##### **equivalent height**

an intrinsic parameter of an electric field (dipole) sensor, which relates the measured voltage across the terminals of the sensor to the E-field component exciting the sensor

#### 3.4

##### **free-field sensor**

an electromagnetic field sensor used at a location distant from any scattering body or ground plane

#### 3.5

##### **high power electromagnetic**

##### **HPEM**

the general area or technology involved in producing intense electromagnetic radiated fields or conducted voltages and currents which have the capability to damage or upset electronic systems. Generally these disturbances exceed those produced under normal conditions (e.g. 100 V/m)

#### 3.6

##### **measurement chain**

one or more electrical devices connected together for the purpose of measuring and recording an electromagnetic signal

#### 3.7

##### **Nyquist frequency**

the Nyquist frequency is the bandwidth of a sampled signal, and is equal to half the sampling frequency of that signal. If the sampled signal represents a continuous spectral range starting at 0 Hz (which is the most common case for speech recordings), the Nyquist frequency is the highest frequency that the sampled signal can unambiguously represent

**3.8****pre-pulse**

refers to a portion of an impulse-like transient waveform that occurs at a time before the time of the primary peak

**3.9****sensor**

a transducer that senses a particular electromagnetic quantity (such as an electric or magnetic field, a current or a charge) and converts it into a voltage or current that can be measured. Typically, this is the first element in a measurement chain for EM measurements

**3.10****waveform norm**

a parameter that is determined from a mathematically well-defined operation on a waveform or signal (such as an integration of the waveform), which yields a scalar number that permits a comparison of various waveforms or their effects

**3.11****waveform parameter(s)**

a single parameter that denotes a waveform characteristic (such as the rise time of the waveform), which is difficult to cast into the waveform norm formalism, yet which is useful in describing a response

**3.12****-dot**

a suffix (as in I-dot), which denotes the derivative with respect to time of the quantity (I), implying that the measurement is proportional to the time rate of rise of the response (I)

## 4 Measurement of high-power transient responses

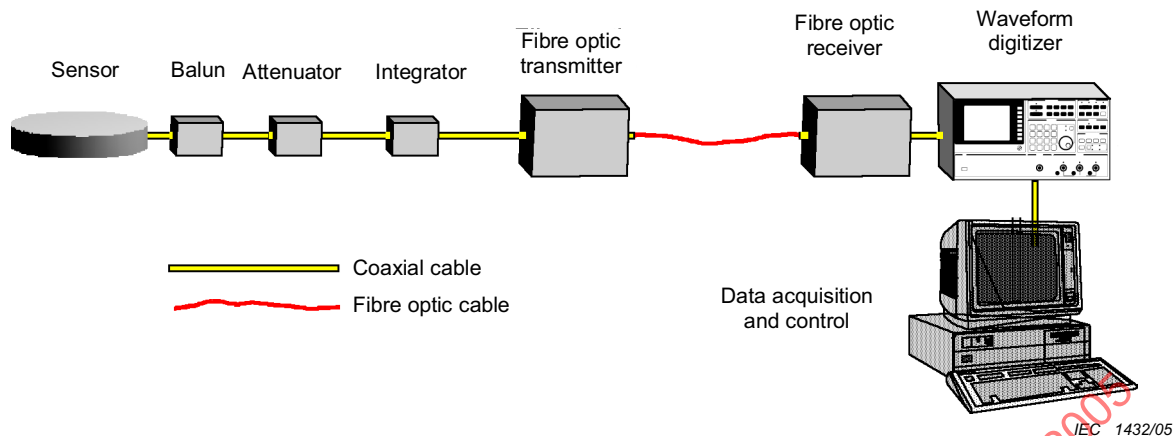
This standard is concerned with the measurement and description of high-power transient signals resulting from a high altitude nuclear detonation (referred to as the high altitude electromagnetic pulse – HEMP) or from the use of a transient source (or pulser) producing high-power electromagnetic (HPEM) fields. Typically, the physical quantities being measured include the electric (E) and magnetic (H) fields in (or near) a facility or test object, or the induced current and charge (or voltage) on conducting wires entering into the facility or test object.

This clause of the standard describes the overall measurement techniques for these transient responses, and in Annex A, suggests several waveform parameters and norms that shall be used to characterize the measured responses. Many of the measurement methods and equipment may also be used for measuring time harmonic (i.e., frequency domain) signals; however, this application is not considered further in this document, as we shall be concerned with only the measurement of transient signals.

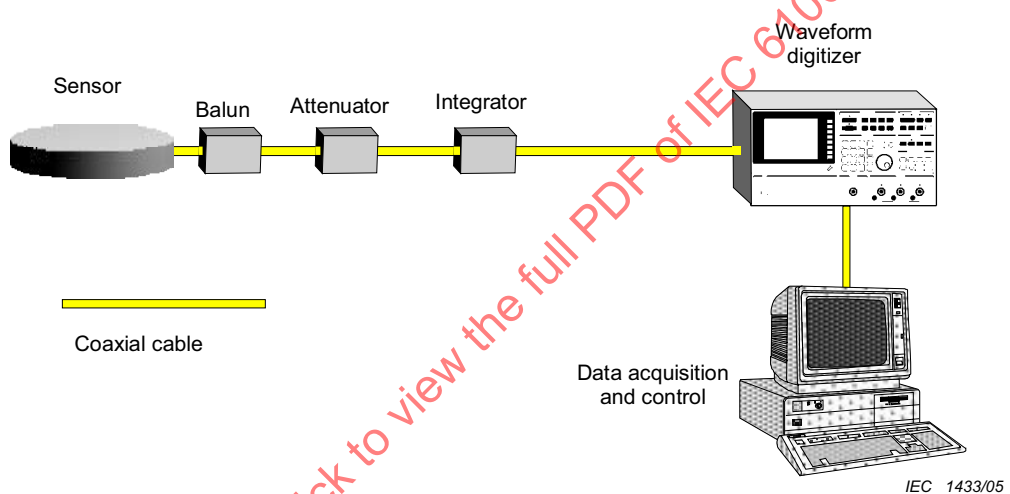
### 4.1 Overall measurement concepts and requirements

The measurement of transient response quantities is realized by using a number of transient signal processing elements linked together in a sequential manner. Referred to as a “measurement chain”, this collection of equipment will detect, process, transmit and record measured transient responses, so that they can be used after the test is finished to analyse a measured quantity or the electrical behaviour of the system under test.

Figure 1 shows two typical instrumentation chains that shall be used for measuring high-power transient responses. The measurement chain shown in Figure 1(a) contains the following elements.



(a) Instrumentation chain using a coaxial cable and fibre optics



(b) Instrumentation chain with only coaxial signal lines

**Figure 1 – Illustration of a typical instrumentation chain for measuring high-power transient responses**

- Coaxial cable – this element provides an electrical connection between the various elements of the measurement chain, at a constant impedance (typically  $50\ \Omega$ ). An alternative to this element is the fibre-optics transmission system discussed below.
- Sensor – a device that converts the measured quantity (EM field, current, or charge) into a voltage that can be measured.
- Balun – a device that operates as a matching transformer to ensure that the sensor is well adapted (matched) to the coaxial signal line. This device also helps to suppress common-mode signals.
- Attenuator – a signal reduction device installed in-line to reduce the sensor signal strength if it is too large.
- Integrator – an active or passive device to integrate in time the sensor output. This is needed because in some cases, a sensor will respond to the time rate of change (e.g., the derivative) of the measurement quantity. (Signal integration can also be performed in software.)
- Fibre optics transmitter – a device to convert the measured fast transient electrical signal to a modulated optical signal, which can be transmitted away from the vicinity of the sensor to a distant recording device.

- Fibre optics cable – a non-conducting fibre cable that can be routed in and around the system under test to permit the transmission of the optical signal to the distant optical receiver.
- Fibre optics receiver – a device that receives the modulated optical signal from the transmitter, demodulates it and recovers the imbedded information from the sensor.
- Waveform digitiser – this is the detector in the measurement chain, which receives the sensor electrical analogue signal, converts it into a stream of digital data and then passes these data on to a recording device.
- Data acquisition and control computer – the main logic processor to conduct the measurements and store and analyse the results.

Additional information on each of these elements in the measurement chain will be provided later in this clause.

Not all of the elements of the measurement chain in Figure 1(a) are always necessary. For example, the attenuator shall be required only if the sensor response is so large that it tends to over-drive the fibre optics (FO) transmitter and cause signal distortions. Similarly, some sensors may have a self-contained integrator, so that the integrator element in the measurement chain shall be omitted.

Figure 1(b) illustrates a case where the entire measurement chain is interconnected only by a coaxial cable. The FO system is not present in this case, perhaps due to some special feature of the signal being measured:

- the dynamic range of the desired signal is larger than that provided by the FO transmit/receive equipment,
- the measured pulse is much faster than the transmission capabilities of the FO system, or
- perhaps the cost of the FO system is prohibitive.

Regardless of the configuration of the measurement chain, there are several basic measurement principles that must be recognized during the course of performing the measurements. These are as follows.

- The measurement sensor always perturbs the EM field in its vicinity (or influences the local current and/or charge densities). It can be shown that if a sensor were designed to not perturb the field, it would register a zero response.
- The use of a measurement chain can “load” the system or circuit being measured, so that the obtained reading may not be the true response.
- The measurement chain can be used to measure both near field and far field responses. Typically, a field sensor will measure only one of the three orthogonal E- or H-field components, and whether the observation point is in the near-zone or the far zone is unimportant in describing the responses. In the far-zone, the E/H ratio of the principal (transverse) field components is equal to the impedance of free-space ( $377 \Omega$ ), but in the near zone this E/H relationship is not maintained.
- The sensor shall be calibrated to provide a suitable relationship between its electrical output and the response quantity it is measuring.
- In addition to the sensor, the remainder of the measurement chain can also add errors to an EM field quantity being measured, and such errors shall be minimized. Such errors can arise both from secondary scattering from the measurement equipment (which adds an error in the fundamental EM field quantities being measured), and from a perturbation of the response provided by the sensor as it propagates through the measurement chain (say, from external common-mode currents on a coaxial cable affecting the internal signal through the shield transfer impedance). The use of the FO transmission system is one way of minimizing this unwanted perturbation. Other ways include a careful routing of the coaxial cable so as to minimize pick-up, the use of ferrite beads on the coax to attenuate induced currents, additional shielding over the coaxial lines, and keeping the length of the coax line as short as possible.

- Calibration procedures shall be applied to all elements of the measurement chain. The integrator functions ideally only over a particular frequency band. The coaxial cable has increasing loss as the frequency increases. Each of these facts shall be taken into account in developing an end-to-end calibration of the measurement chain.
- The measurement system noise shall be determined and its effects on the measured response quantities shall be quantified.
- Once a “raw” waveform is measured and digitised by the recording device, the calibration function shall be applied and a “corrected” response waveform determined.
- After the corrected waveform is determined, it shall be summarised by one or more waveform parameters, or norms, identified in Annex A.

Details and requirements for each of these measurement chain elements will be discussed in 4.3.

#### 4.2 Representation of a measured response

The measured, corrected and digitised waveform that is ultimately recorded by the data acquisition computer is usually a complicated function of time. To easily distinguish between one waveform and another, and to relate a particular waveform to a possible effect on a system or facility, one or more scalar numbers representative of the waveforms shall be used. In this manner, only a few numbers, as opposed to the entire data record of the transient waveform, can summarize the essence of a waveform.

In describing the response waveform in this manner, there are two classes of numbers that shall be used. Waveform parameters are numbers that are immediately obvious from an examination of the transient response, such as the peak amplitude. Waveform norms, on the other hand, are mathematically defined scalar parameters that require a numerical processing of the total waveform. The energy contained in the waveform is an example. In this clause of the standard, each of these types of waveform parameters is defined.

Annex A of the present standard provides additional information on how measured transient waveforms can be characterized.

#### 4.3 Measurement equipment

As noted in Figure 1 there are four major elements to the measurement system. These include:

- the response sensor that measures an electrical parameter (EM field component, a current, or a charge) and converts it into a voltage;
- the transmission system that transports the measured voltage from the sensor to the detection equipment;
- the detection (or digitisation) system that takes the received voltage response and converts it into a digital format for processing and storage; and
- the computer controlling the measurement process and performing data processing and storage.

##### 4.3.1 The measurement chain

Each of these measurement chain elements can affect the amplitude and wave shape of the recorded signal, and it is important to understand and control such perturbations. As an example, consider the case of a transient EM field described by its E-field component  $E_o(t)$  striking the field sensor in Figure 1(a), and producing a transient response at the recording device given as  $R_{\text{measured}}(t)$ . As noted in [1]<sup>1)</sup>, the relationship between the transient response and excitation is given by a convolution (\*) operation as

<sup>1)</sup> Figures in square brackets refer to the Bibliography.

$$R_{\text{measured}}(t) = E_o(t) * T(t), \quad (1)$$

where  $T(t)$  is the impulse response of the measurement system. Given the measured response  $R_{\text{measured}}(t)$ , the goal is to determine the excitation  $E_o(t)$ , and [1] represents this process symbolically as the deconvolution (1/\*) operation

$$E_o(t) = R_{\text{measured}}(t) (1/*) T(t). \quad (2)$$

In [1], various techniques that may be used to evaluate this deconvolution operation to determine  $E_o(t)$  are discussed, with one of them being recasting equations (1) and (2) in the frequency domain through the use of Fourier transforms, and then using the transfer function concept [2] to deconvolve the excitation function.

Denoting the Fourier transforms of the measured transient response and the excitation E-field at the sensor by  $\tilde{R}_{\text{measured}}(f)$  and  $\tilde{E}_o(f)$ , respectively (see Annex A), the frequency domain equivalent of equation (1) is expressed as

$$\tilde{R}_{\text{measured}}(f) = \tilde{T}(f) \tilde{E}_o(f), \quad (3)$$

where now the convolution operation becomes a simple multiplication by the Fourier spectrum of the transfer function  $\tilde{T}(f)$ . In the frequency domain, the deconvolution operation of equation (2) is given as the inverse of equation (3) as

$$\tilde{E}_o(f) = \tilde{T}(f)^{-1} \cdot \tilde{R}_{\text{measured}}(f). \quad (4)$$

NOTE In this standard, transient quantities are represented using the notation  $F(t)$ , and the corresponding Fourier spectral density is  $\tilde{F}(f)$ .

This deconvolution is easily carried out, as long as the transfer function spectrum  $\tilde{T}(f)$  is not zero at any real frequency  $f$ . Once the spectrum of the excitation field is determined, the transient behaviour of this field component may be determined by taking an inverse Fourier transform.

As noted in Figure 1(a), the measurement chain consists of several different elements, each of which contributes to the overall transfer function  $\tilde{T}(f)$ . Because each element in the chain is designed to function at a constant impedance level (typically 50 ohms), the end-to-end transfer function of the measurement chain  $\tilde{T}(f)$  can be evaluated as the product of individual complex-valued, frequency dependent transfer functions for each element in the measurement chain. In this manner, the overall transfer function is given as

$$\tilde{T}(f) = \tilde{T}_{\text{digitiser}}(f) \cdot \tilde{T}_{\text{fibre optics}}(f) \cdot \tilde{T}_{\text{integrator}}(f) \cdot \tilde{T}_{\text{attenuator}}(f) \cdot \tilde{T}_{\text{balun}}(f) \cdot \tilde{T}_{\text{sensor}}(f). \quad (5)$$

To determine the spectrum of the excitation field from equation (4) it is necessary that the transfer function  $\tilde{T}(f)$  be known. Methods for determining this transfer function accurately (both in magnitude and phase over a wide frequency range) will be discussed in Clause 6 of this standard. In many instances, however, the various transfer function components in equation (5) are designed to be very simple functions of frequency or even constants over a wide frequency band, and this makes the overall transfer function very simple.

Subclause 4.3.2 in this standard and Annex B discuss several different types of sensors that provide output responses that are related to an excitation function (like an incident field or induced current.) The responses of these sensors are seen to be of two basic types: one which has an output that is approximately proportional to the excitation quantity and another,

in which the sensor output response is proportional to the time rate of change (derivative) of the excitation.

For the first type of sensor, the transient response of the device is given as

$$V_{\text{out}}(t) = K_{\text{sensor}} E_o(t) \quad (6a)$$

and the corresponding frequency domain spectral representation is

$$\tilde{V}_{\text{out}}(f) = K_{\text{sensor}} \tilde{E}_o(f), \quad (6b)$$

where  $K_{\text{sensor}}$  is a characteristic constant of the sensor.

For the second type, or differentiating sensor, the output is given as

$$V_{\text{out}}(t) = K_{\text{sensor}} \frac{d}{dt} E_o(t), \quad (7a)$$

and the frequency domain spectrum is

$$\tilde{V}_{\text{out}}(f) = j 2\pi f K_{\text{sensor}} \tilde{E}_o(f). \quad (7b)$$

For the case when a differentiating sensor is used, it is necessary to provide some sort of an integration function to recover the excitation function from the derivative signal provided by the sensor. This can be provided either by an integrating circuit element in the measurement chain (described more fully in 4.3.5), or by a post-processing of the computed response using numerical methods. If a hardware integration of the signal is to be used, the integrator provides an output that is proportional to the integral of the input signal, and in the frequency domain, this is expressed as

$$\tilde{V}_{\text{out}}(f) = \frac{1}{j 2\pi f} K_{\text{integrator}} \tilde{V}_{\text{in}}(f), \quad (8)$$

where  $K_{\text{integrator}}$  is a characteristic constant for the integrator component.

Thus, when a differentiating sensor is used in the measurement chain, the measured response from equation (3) can be represented as

$$\begin{aligned} \tilde{R}_{\text{measured}}(f) &= \tilde{T}(f) \tilde{E}_o(f) \\ &\approx \left( K_{\text{digitiser}} \cdot K_{\text{fibre optics}} \cdot \frac{1}{j 2\pi f} K_{\text{integrator}} \cdot K_{\text{attenuator}} \cdot K_{\text{balun}} \cdot j 2\pi f K_{\text{sensor}} \right) \tilde{E}_o(f) \quad (9a) \\ &\approx K \tilde{E}_o(f) \end{aligned}$$

and if a self-integrating sensor is used, the measured response is

$$\begin{aligned} \tilde{R}_{\text{measured}}(f) &= \tilde{T}(f) \tilde{E}_o(f) \\ &\approx \left( K_{\text{digitiser}} \cdot K_{\text{fibre optics}} \cdot K_{\text{attenuator}} \cdot K_{\text{balun}} \cdot K_{\text{sensor}} \right) \tilde{E}_o(f) \quad (9b) \\ &\approx K \tilde{E}_o(f) \end{aligned}$$

The scalar coefficients of the components ( $K_i$ ) in equations (9a) and (9b) are typically provided by the manufacturers of the measurement chain components and are often used without further calibration. However, for accurate measurements of such HPEM fields, each of these components shall be calibrated before being used in a measurement program.

Regardless of the type of sensor used in the measurement, the overall transfer function  $K$  is used to compute the excitation function spectrum as

$$\tilde{E}_o(f) = K^{-1} \cdot \tilde{R}_{\text{measured}}(f). \quad (10)$$

Because  $K$  is frequency independent, the resulting transient response is given as

$$E_o(t) = K^{-1} \cdot R_{\text{measured}}(t). \quad (11)$$

In many practical cases involving transient signals having fast rise times, the frequency range of interest is such that the transfer function  $\tilde{T}(f)$  is not a constant over the frequency band. Consequently, equations (10) and (11) are not suitable for determining the excitation from the measured response. In such cases, it shall be necessary to determine the overall complex-valued transfer function of the measurement chain by calibration methods, and then use equation (4) to compute the excitation function.

#### 4.3.2 Response sensors

As discussed in 4.3, the first element in the measurement chain of Figure 1 is the EM sensor, which interacts with the local EM field (or current, or charge) and produces a voltage output. The design of a sensor has been described in detail by Baum [3, 4], where the following requirements are set out for an “ideal” sensor.

- a) It is an analogue device which converts the electromagnetic quantity of interest to a voltage or current (in the circuit sense) at some terminal pair for driving a load impedance, usually a constant resistance appropriate to a transmission line (cable), terminated in its characteristic impedance.
- b) It is passive.

NOTE As discussed in Annex B, it is also possible to have sensors that are active; however, the passive sensor is viewed as being simpler to calibrate, and thus, are often viewed as being more desirable than the active sensors.

- c) It is a primary standard in the sense that, for converting fields to volts and current, its sensitivity is well known in terms of its geometry; i.e., it is “calibratable by a ruler” [5]. The impedances of loading elements may be measured and trimmed. Viewed another way, it is, in principle, as accurate as the standard field (voltage, etc.) in a calibration facility. (A few percent accuracy is usually easily attainable in this sense).

NOTE This requirement is for the “ideal” sensor, in which there is a simple geometrical relationship between the field component being measured and its output signal. This simplifies the sensor calibration procedures. For other types of sensors that are not “calibratable by the ruler”, the calibration process must be accomplished as described in 6.2.2.

- d) It is designed to have a specific convenient sensitivity for its transfer function, which is often expressed as an equivalent area or an effective height.
- e) Its transfer function is designed to be simple across a wide frequency band. This may mean “flat”, in the sense of volts per unit field or rate of rise of the field, or it may mean some other simple mathematical form that can be specified with a few constants (in which case more than one specific convenient sensitivity number is chosen).

In using such sensors, it is important to keep in mind that there can be significant voltages developed within the sensor and on the sensor cables. If the quantity being measured is too large for the sensor design, there can be corona or arcing within the sensor, which will cause a misreading of the response, or possibly damage within the sensor. Thus, the sensor shall be carefully selected for the expected response level to be measured.

Annex B provides more details on the representations of the transfer functions for different types of EM field sensors. Additional details of the physical realization of sensors also are provided in Annex C of IEC 61000-4-23.

#### 4.3.3 Baluns

When a balanced EM sensor, like a dipole antenna, is fed with coaxial cable, it is possible that a portion of the induced antenna current will flow on the exterior surface of the cable shield. Such currents can flow around the outside cases of measurement equipment and couple energy into the power lines or into the ground connection. This can result in unpredictable equipment performance and unintended interference to other equipment. Figure 2 illustrates such a connection, where it is evident that a portion of the current from the sensor ( $I_{out}$ ) flows in an uncontrolled manner on the exterior of the coaxial cable and the equipment enclosure.  $I_{out}$  can also be considered to be the common mode portion of the cable current.

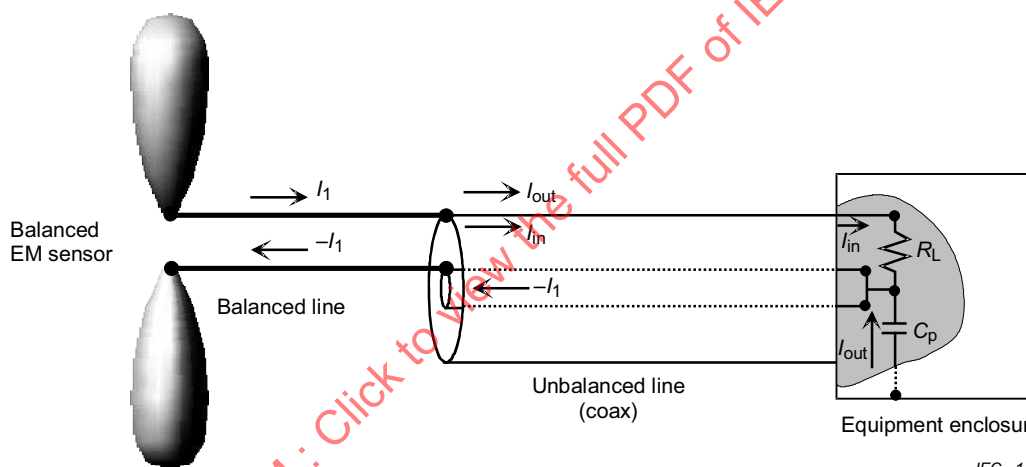


**Figure 2 – Illustration of a balanced sensor and cable connecting to an unbalanced (coaxial) line where  $I_{out} + I_{in} = I_1$**

The balun prevents the current  $I_{out}$  from flowing on the cable exterior, and helps to preserve the antenna and feedline current balance. As such, it provides a high impedance for the common mode currents flowing on the transmission line structure, while at the same time permitting the differential mode currents to flow unimpeded.

There are many different designs for baluns, some of which are based on resonance characteristics of transmission lines (and consequently, are narrow-band in their operation) and others are wide band devices. Often, ferrite chokes can be used to minimize unwanted common mode currents on the balanced line. For transient measurements, baluns must be wideband in order to adequately maintain the waveform of the EM field being measured.

Figure 3 presents the electrical configurations of several different types of baluns. Balun (a) in the figure is constructed of a  $\lambda/2$  delay line, and as a consequence it is a narrow-band balun. It is connected between the two balanced-line terminals as shown in the diagram, and forces the line voltages to ground to be equal and opposite at the design frequency. A balanced-to-unbalanced impedance ratio of 4 is obtained with this balun.

The other four baluns in Figure 3 operate over a wide band of frequencies. Balun (b) is constructed from helically wound transmission lines that are connected in parallel at the unbalanced end. Sufficient line length is used to develop high impedances to permit grounding at the opposite ends of the coils, where the two lines are connected in series to form the balanced terminals. A balanced-to-unbalanced impedance ratio of 4 is provided by this balun.

An example of a frequency-independent balun is shown in part (c) of the figure. Two coaxial lines are connected in parallel at the unbalanced terminal and in series at the balanced terminal. A third cylindrical conductor cylinder is added to preserve symmetry. The impedance transformation ratio for this balun using 2 coaxial cables is 4. More coaxial lines could be added in parallel to give impedance transformation ratios of 9, 16, etc.

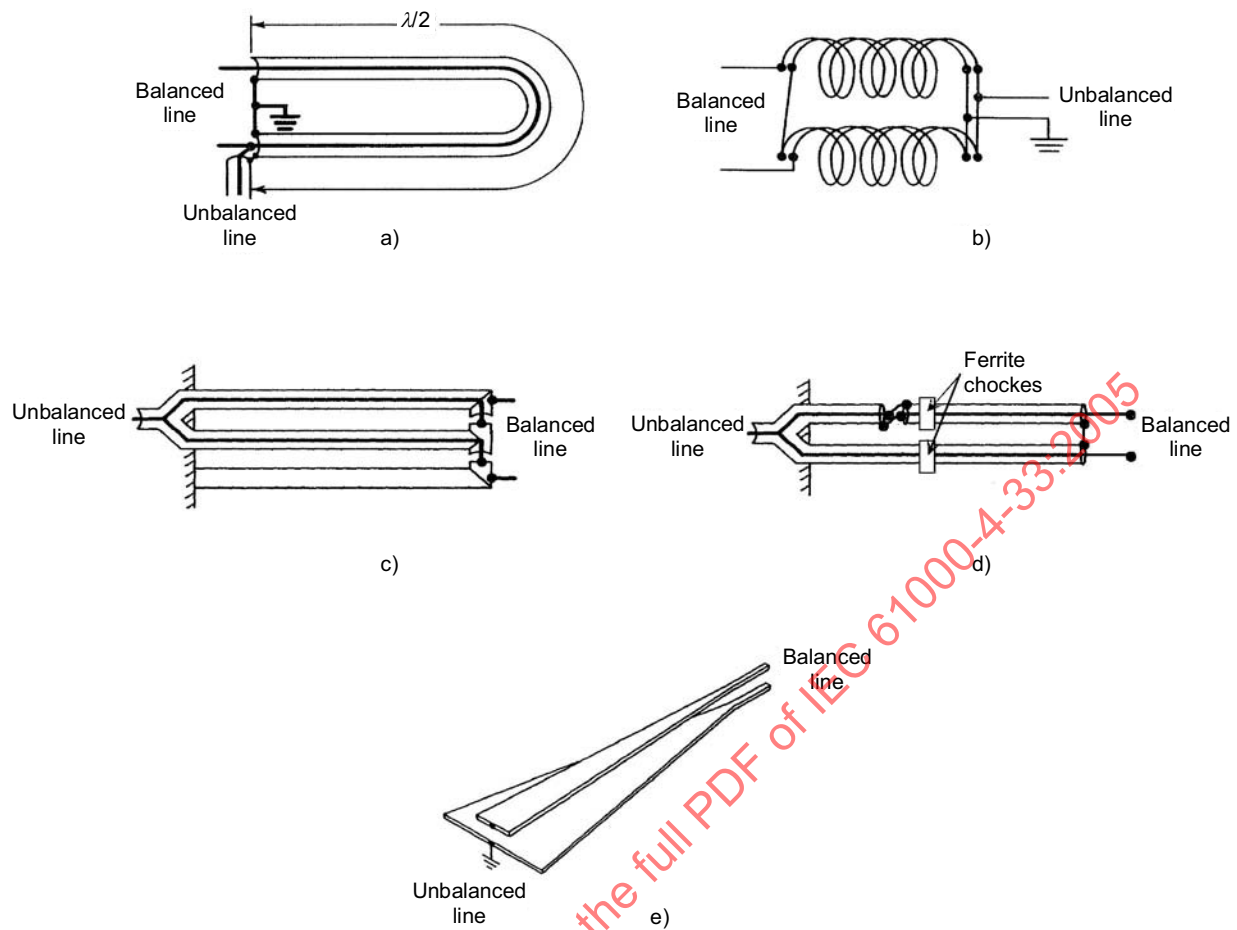
The balun in part (d) of the figure uses only two coaxial cables, one of which has the inner and outer conductors reversed. Two ferrite chokes are added to the coax exteriors to eliminate common mode currents.

The balun in part (e) of Figure 3 is a very wide band device, consisting of a tapered transmission line that converts gradually from an unbalanced line to balanced line. The length of the transition section shall be greater than  $\lambda/2$  at the lowest frequency of interest. In this device, the impedance of the balanced (stripline) and unbalanced (coax) sections can be different, with a slow variation from one to another provided by the geometry of the transition section.

There are several practical details that must be taken into account when specifying a balun for use in a measurement system. These include the following:

- the bandwidth of the balun;
- the change of impedance level, if any, from the balanced to unbalanced ports;
- the effective “attenuation” of the signal level due to the insertion of the balun;
- the maximum power rating of the device.

These data are typically provided by the balun manufacturer. More complete information, such as a frequency sweep of the balun signal throughput (in magnitude and phase) are rarely provided, and if these characteristics are needed to be included in a highly accurate model of the instrumentation chain, such responses must be measured by the user.



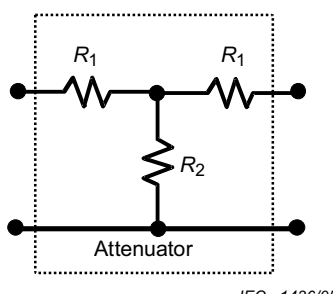
IEC 1435/05

Figure 3 – Examples of some simple baluns [4b]

#### 4.3.4 Attenuators

Another component shown in the measurement chain of Figure 1 is the attenuator. At times, a measured signal may be too strong and a reduction of its amplitude will be needed to avoid saturation of the measurement equipment. To do this, an attenuator will be used.

As shown in Figure 4, an attenuator is a resistive ladder, which is designed to provide a reduction of the signal amplitude, while at the same time, maintaining a constant impedance matching to the line. Typically, these are designed to be used in  $50\ \Omega$  cable systems, and the attenuation is specified in dB.



IEC 1436/05

Figure 4 – A typical circuit for an in-line attenuator in the measurement chain

As with the other components in the measurement chain, the specified attenuation of the device is only nominal. Figure 5 presents a measured attenuation of a specified 20 dB attenuator for a 50- $\Omega$  system over a frequency range from 1 MHz to 1 GHz. Not shown in this figure is the corresponding phase of the attenuation factor, which must also be used in any end-to-end model of the measurement chain.

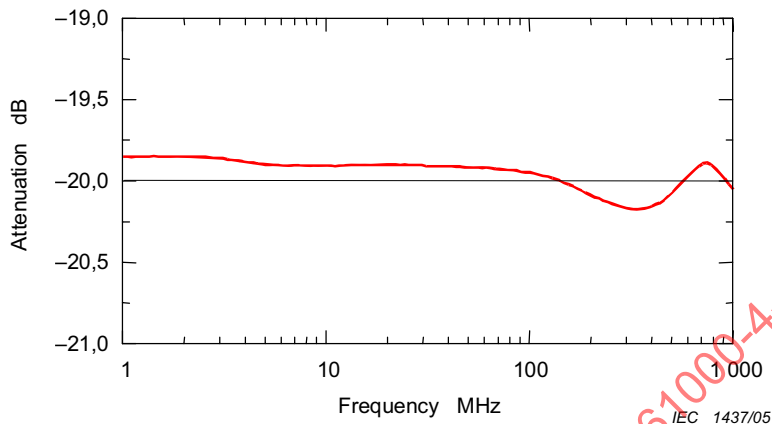


**Figure 5 – Illustration of the typical attenuation of a nominal 20 dB attenuator for a 50- $\Omega$  system, as a function of frequency**

In the selection of an attenuator for the measurement chain, the following parameters shall be used:

- nominal attenuation;
- impedance level for the attenuator;
- maximum working peak voltage (or power);
- effective bandwidth of the device.

As in the case of the balun, these parameters are usually provided by the manufacturer. However, detailed frequency sweeps of the attenuation magnitude and phase are usually not provided and they need to be measured.

#### 4.3.5 Integrators

Because the output response from a derivative (rate of rise) sensor is proportional to the time rate of change of the measured quantity, it is necessary to use an integrator to obtain the correct current waveform. Such integrators can be either passive or active.

**NOTE** Of course, this integration could also be performed numerically on the measured derivative data. However, doing this can cause problems with baseline shifts, which arise from uncertainties in the DC component of the field being measured.

A passive integrator is essentially a resistor/capacitor network, as shown in Figure 6. These components are most suitable for large amplitude, fast rise-time pulses, since they require a high voltage from the derivative sensor to give acceptable accuracy of the output response. Furthermore the low-frequency sensitivity of such a measuring system (derivative sensor plus integrator) is poor. Typically, such integrators have been used with HEMP and lightning test equipment, and with rail gun measurements. A notable advantage of these components is that they are passive and do not require external power.

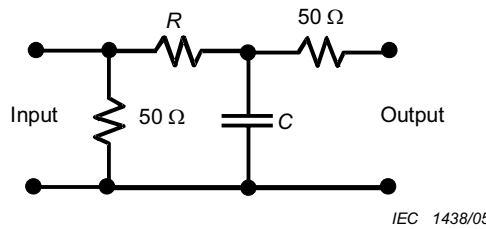


**Figure 6 – Typical circuit diagram for an in-line integrator**

The passive integrator is characterized by its time constant ( $RC$ ), where  $R$  is the integrating resistor and  $C$  is the integrating capacitor. By using different values of  $R$  and  $C$  the characteristics of the complete transducer (derivative sensor plus integrator) can be varied over an enormous range. For example a typical flexible coil can be used to make current measurements from a few mA to more than 1 MA simply by changing these two components in the integrator.

The transfer function for the voltages across the input and output of the integrator will typically be described by the expression

$$\frac{\tilde{V}_{out}}{\tilde{V}_{in}} = \frac{1}{1 + j2\pi fRC} \quad (12)$$

Common  $RC$  time constants are 1, 5, 10 and 100  $\mu$ s. Values of  $R$  are 1, 5, 10 and 100  $k\Omega$ , respectively, and  $C$  is 1,0 nF. The specified load impedance for such integrators is typically a high impedance load (resistance  $>1 M\Omega$ , capacitance  $<10 pF$ ). Many measurement devices have a 50  $\Omega$  input resistance only, and if these latter components are used with the integrator, the responses will be in error. The user must be certain that a high impedance measurement device is used. Figure 7 presents the integrator transfer function ratio magnitude  $|V_{out}/V_{in}|$  for the aforementioned integrator time constants, with the frequency range of integration action shown in the figure.

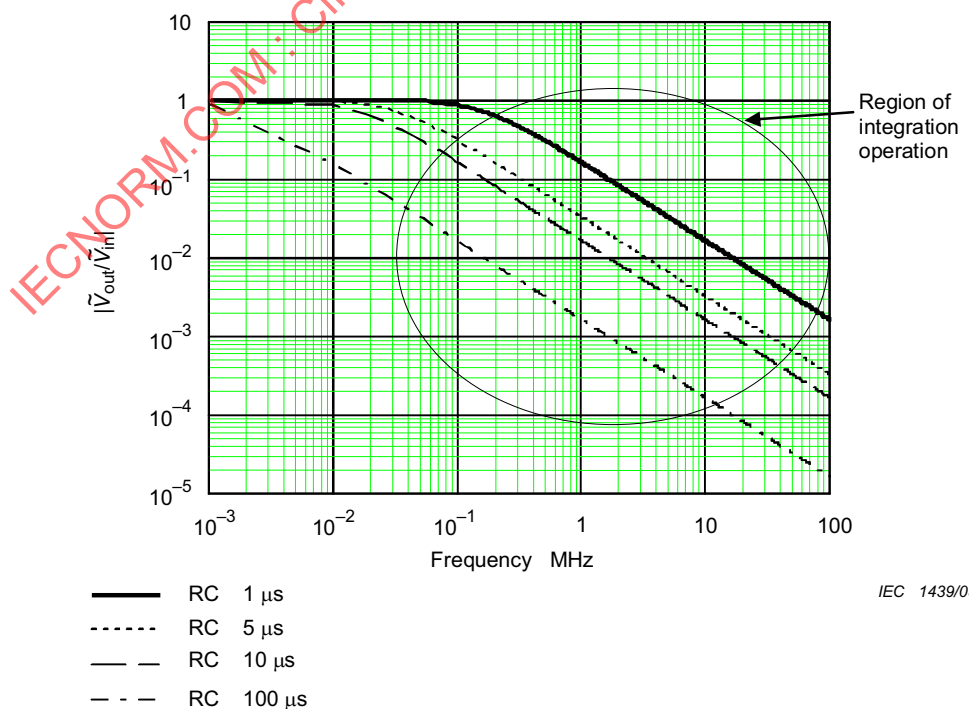


**Figure 7 – Plot of the transfer function of the integrating circuit of Figure 6**

Active integrators are generally much more versatile than are the passive integrators. They can be used both for low currents (less than 1 A) and at low frequencies (less than 0.1 Hz), as well as for currents of more than 1 MA and at frequencies approaching 100 MHz. The low-frequency performance of this integrator is determined by the integrator design.

#### 4.3.6 Interconnecting transmission links

As noted in Figure 1, the various components of the measurement chain can be interconnected either by a coaxial cable or by a fibre optic transmission link. Both of these transmission paths also affect the signal being measured and ideally, they shall be included in any correction made to the measured signal. Ideally, these signal paths are designed to operate without signal attenuation or distortion, but in actual practice, there is an effect on the signal quality when these components are used.

##### 4.3.6.1 The coaxial cable link

Considering the coaxial cable transmission path, there can be losses within the metal conductors of the cable and dielectric losses. The effects of these losses is to provide a frequency dependent signal in the cable, and this results in an attenuation of a wave travelling down the line, and in most cases, a dispersion of the signal waveform. That is to say, the waveform of the travelling wave will broaden and become distorted as it propagates down the line.

While such loss effects can be computed using appropriate models for the coaxial cable, characterising the cable through measurements is more accurate, since the frequency dependent behaviour of the cable dielectric constant and conductivity is usually unknown. As an example of some typical cable losses as a function of frequency, Figure 8 presents measured per-unit-length transmission (in units of dB/m) for a “normal” coaxial cable, and a high-quality copper cable, which is more suited for high frequency measurements. Note that in both cases there is a decreasing transmission (e.g., increasing attenuation) of the cable as the frequency increases. As in the case of other measurement chain components, this transmission function is really a complex-valued quantity and this complex function must be used in incorporating the cable attenuation effects in the overall measurement chain.

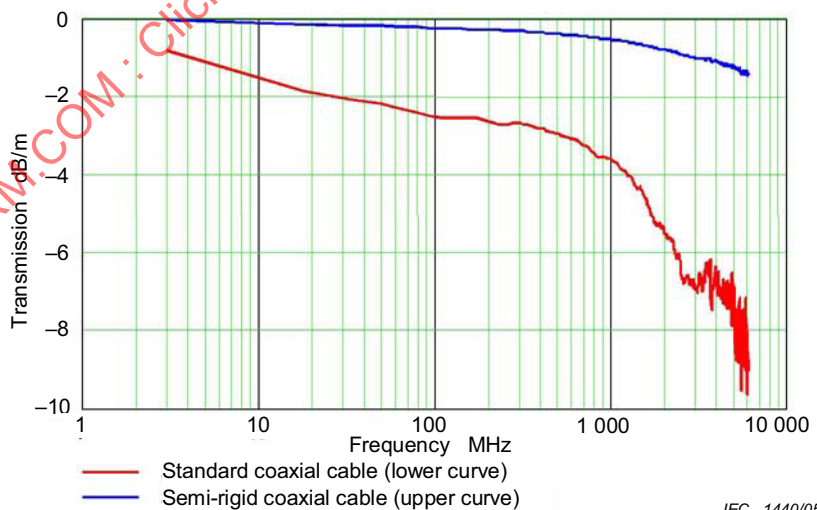


**Figure 8 – Illustration of the frequency dependent per-unit-length signal transmission of a standard coaxial cable, and a semi-rigid coaxial line**

#### 4.3.6.2 The fibre optic link

An alternative to a coaxial, or “hard-wired” link of equipment in the measurement chain is the fibre optic link. As noted in Figure 1 this consists of a transducer that converts an electrical signal to an optical signal (the “transmitter”), a fibre optics cable that transmits the optical signal over some distance and another transducer (the “receiver”), which converts the optical signal back to an electrical signal. The benefit of this system is that the fibre optic cable is, in principle, non-conductive. This eliminates a possible inadvertent signal propagation path that would be present if the coaxial line were to be used, thereby reducing the influence that the measurement system has on the normal EM environment in the vicinity of the measurement chain.

NOTE Some fibre optic cables have an exterior armor made of conducting material for physical protection. These types of cables shall be avoided for HPEM measurements.

While the use of fibre optics links provides certain benefits in electrically isolating the measurement equipment, its use can provide some problems. The transducers typically require external power in the form of batteries, and this can add unwanted interruptions in a measurement campaign when the batteries need replacement. More serious, however, is that the transducer equipment will add to the system noise and reduce the bandwidth of the measurement chain.

#### 4.3.7 Recording equipment

The transient HPEM waveforms are typically measured using a digital oscilloscope or a waveform digitiser. Consult 6.1.2 and 6.2.2 of IEC 61000-4-25 for additional requirements for this equipment.

#### 4.3.8 Equipment layout

An important issue in performing HPEM measurements is in the layout of the measurement equipment. As mentioned in 4.1, an EM field sensor always will perturb the incident field. This is an unavoidable consequence of measuring the field. However, the calibration of the sensor takes into account this field perturbation, and the sensor output ultimately provides an indication of the incident, unperturbed field.

A realistic measurement system has other components besides the sensor (see Figure 1) and if these are metallic in any way, they have the possibility of interacting with the incident field and providing additional EM field components at the sensor. Thus, the presence of these components can perturb the local field measured by the sensor and give rise to errors in the measured responses.

The interaction of the incident field with the other components in the measurement chain also can affect the functioning of the components themselves. Consider the case of an incident field acting on a coaxial cable that transmits a measured signal from a sensor to a recorder. This external field can induce currents on the cable exterior, and by virtue of the shield transfer impedance and admittance, an internal voltage source can be induced in the internal signal wire. This source is effectively a “noise” or interference source, and it will modify the sensor signal being transmitted by the cable. Such interference can be eliminated by several means, including using a better shield on the coax, routing the cable in such a way as to eliminate the external EM coupling to the cable, by adding ferrite elements on the cable exterior, or by using fibre optics instead of the coax.

In addition to interacting with the EM field environment and perturbing the observed response, the measurement chain can affect the measurements in other ways. For example, consider the cable current sensor shown in Figure B.7 of Annex B. The presence of this sensor near the cable can load the cable with an effective impedance element, and thereby cause a decrease in the cable current. Thus, although the current read by the probe is “formally” correct, it is not the current that would flow in the cable if the probe were not there. Another example is when one measures a field component in a high Q cavity (e.g. a reverberation chamber).

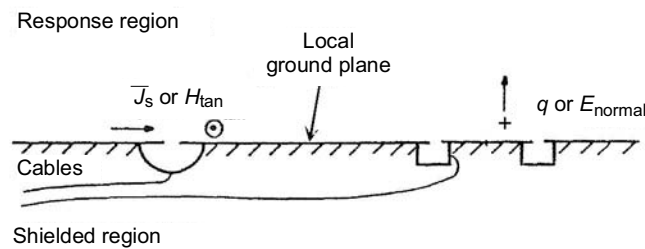
In this case, the probe loads the chamber, resulting in a lower global field level (i.e. not only close to the probe) than what would be found without the probe in the chamber. Again, one measures the true field level, but it is not the field level that was there before the probe was introduced.

A number of practical suggestions regarding sensor and cable positioning have been provided in [6], and these are summarized here. An important consideration in locating sensors, cables and equipment is to do so with minimal impact on the fields being measured. The electrical cables connecting free-field sensors to the measurement chain can significantly perturb the field being measured (unless fibre optics are used) and these types of measurements are not recommended. What is recommended is to use a surface-mounted sensor for the current or charge on a conducting surface that is a component of the object under test. In this manner, the sensor cables can be routed to the measurement equipment by cables in the underside of the ground plane where the EM fields are very small. Such a cabling configuration is shown in Figure 9(a).

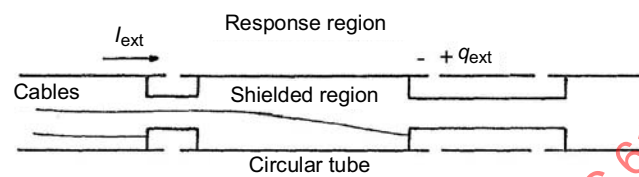
Similarly, when the current or charge on a cylindrical or tube-like conductor is required, the cables shall be routed within the conductor, as indicated in Figure 9(b). For current measurements inside such a cylindrical region, the configuration of Figure 9(c) shall be applied.

At times, however, routing the cable through the local ground plane into the field-free region may not be possible. When this is the case, the cables shall be mounted in the external region (with large EM field strengths), but with special attention paid to the cable routing and bonding to the ground plane. For a surface mount sensor, as shown in Figure 10(a), the shield of the cable linking the sensor and the measurement equipment shall be bonded electrically (using copper adhesive tape) to the ground plane. In addition, the sensor mounting plate shall be bonded to the ground plane.

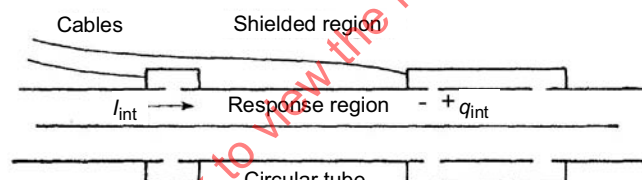
When cable current or voltage measurements are to be made, the cable configurations shown in Figure 10(b) and (c) shall be used. In both cases, the cable shield is again bonded to the local ground plane, and the portion of cable running from the ground plane to the cable shall be made as short as possible. In addition to bonding the cable to the ground plane, it is also possible to consider placing ferrite toroids over the cable shield at convenient locations along the cable to reduce the unwanted current flow on the cable exterior. This is illustrated in Figure 10(b).



a) Cables located below ground plane



b) Cables located inside measurement surface

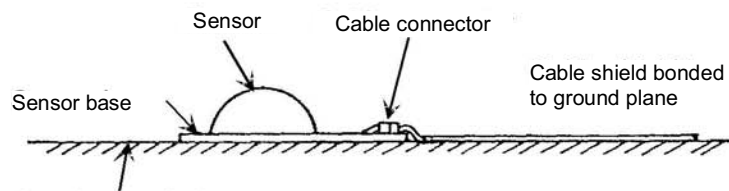


c) Cables located outside measurement surface

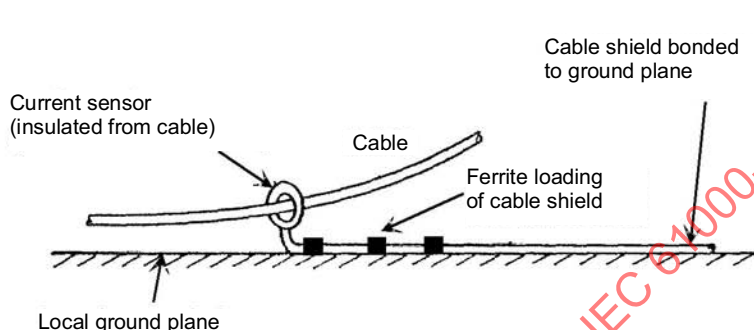
IEC 1441/05

Figures show cross sectional views of a plane, (a), or cables, (b) and (c).

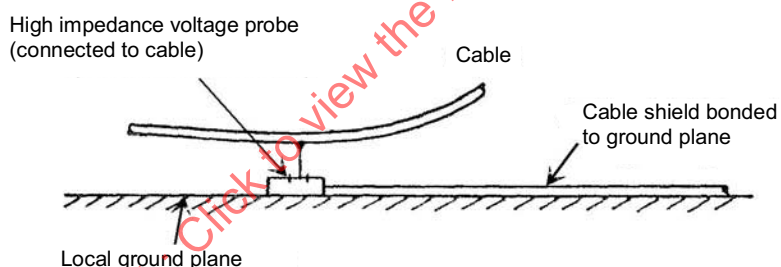
**Figure 9 – Illustration of sensor cable routing in regions not containing EM fields**



a) Connection of a surface field sensor



b) Connection of a surface current sensor



c) Connection of a cable voltage probe

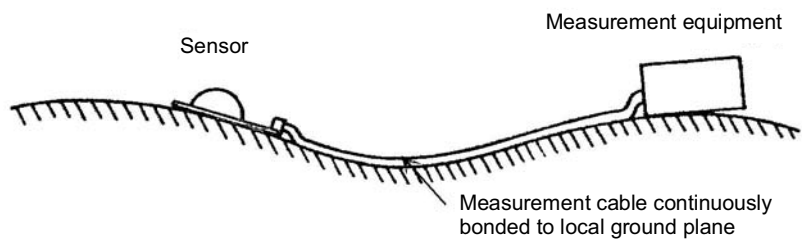
IEC 1442/05

**Figure 10 – Treatment of sensor cables when located in a region containing EM fields**

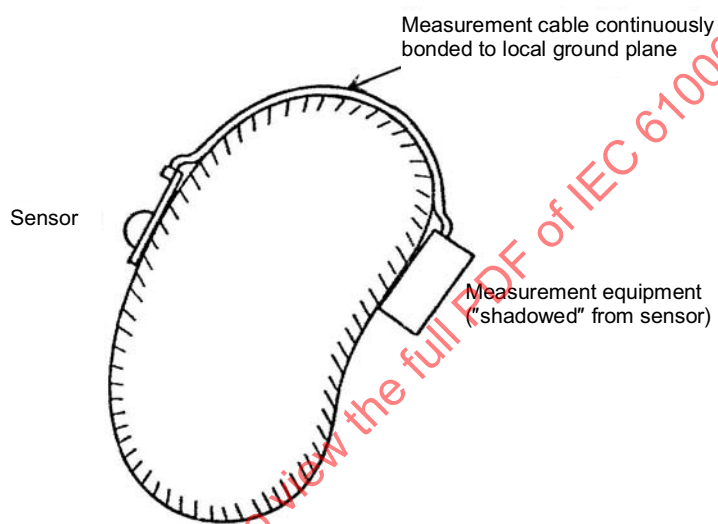
On real systems, the local ground plane may not be perfectly flat, as suggested in Figure 11(a). In these cases, the cable shall be mounted conformally on the local ground, with electrical bonding, if possible, between the cable shield and surface. A further possibility for avoiding perturbations of the EM field by the measurement equipment is shown in Figure 11(b). Here the measurement equipment is located in a region that is effectively isolated from the sensor by the body under test. Of course, the cable shield shall be bonded to the surface.

**NOTE** The large X's on the left figures are intended to indicate an incorrect cable routing.

Figure 12 illustrates several cable routing configurations that shall be avoided in measurements. Figure 12(a) shows a cable passing close to an aperture in the wall of a system being measured. EM fields passing through the aperture will excite the cable shield and this can lead to unwanted responses within the measurement system. Similarly, in Figure 12(b), a cable is allowed to pass from the equipment being measured to another without being bonded to the surfaces. This creates a large loop, which can couple to EM fields in the vicinity of the equipment, thereby causing spurious responses in the measurements.



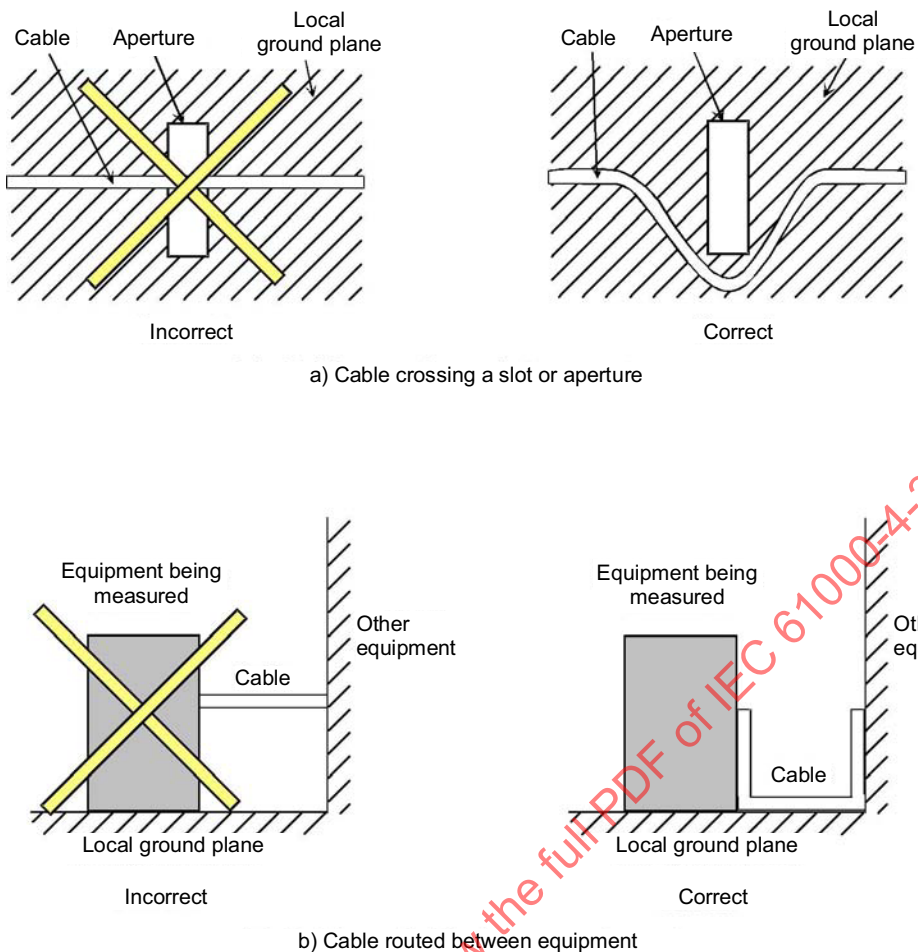
a) Conforming the measurement conductors to local geometry



b) Minimising measurement equipment interference on sensor operation

IEC 1443/05

**Figure 11 – Conforming cables to local system shielding topology**



IEC 1444/05

NOTE The large X's on the left figures are intended to indicate an incorrect cable routing.

**Figure 12 – Correct and incorrect methods of cable routing**

#### 4.4 Measurement procedures

Consult Clause 8 of IEC 61000-4-25 for requirements for measurement procedures. Annex C of the present standard contains additional information regarding HPEM measurement procedures.

#### 5 Measurement of low frequency responses

Low frequency signals having spectral components on the order of several hertz are also of concern for HPEM measurements. These signals arise in the late-time EMP environments, which are similar to the electric and magnetic fields on the earth surface produced by geomagnetic storms.

Because the HPEM environments are so similar to these naturally occurring disturbances, many of the same measuring techniques used for geomagnetic storm effects can be used. These include measurements of the transient behaviour of magnetic fields on the earth surface and voltages and currents in long conductors that are connected to the earth. Clause B.9 discusses various aspects of sensors that are suitable for conducting such low frequency measurements.

## 6 Calibration procedures

The calibration of a measurement channel can be obtained by several methods, ranging from very accurate measurements that are traceable to standard EM fields, to approximate schemes that require simple attenuation factors and other scalar numbers to characterize the components in the system. This clause discusses general calibration procedures, but does not describe calibration methods in detail.

The requirement for using one method over another depends on the type of measurement being performed. For example, if a radiated emission level test is considered to verify compliance with an EMC specification, it is not necessary to have a phase coherent measurement. Furthermore, for many applications, a set of constant magnitude calibration functions may be permissible. On the other hand, if a fast-rise HPEM transient measurement is required, or conversely, if a wide-band CW measurement for reconstructing a HPEM transient response is needed, it is crucial that both magnitude and phase information be maintained in the measurements. This implies that any calibration functions must be complex-valued.

Unfortunately, most EM field sensors and other measurement chain components are specified by magnitude-only data from the manufacturers. Furthermore, some commonly available measurement software will not permit the possibility of using complex-valued transfer functions or correction factors. Users of this equipment and software are cautioned to carefully examine their test requirements to ensure that the use of these data will not add undue errors to their test results.

There are two basic approaches for calibrating a measurement chain. One is to consider the entire chain as a single component and perform a calibration measurement on this ensemble. The other approach is to develop a model of the calibration chain, consisting of the sensor or probe, attenuators, filters, transmission lines, etc., and to calibrate each component independently. Then, the individual calibration factors may be combined analytically to provide the overall calibration function for the entire measurement chain.

In this clause, the above-mentioned concepts for calibration are discussed.

### 6.1 Calibration of the entire measurement channel

#### 6.1.1 Direct calibration

Several different approaches can be used to calibrate the entire measurement chain. For the calibration of a single measurement chain, such as that shown in Figure 1, the simplest approach is to locate the sensor in a known electromagnetic field environment and to make a note of the reading of the detector. By varying the frequency of the EM environment, the frequency dependence (both in magnitude and phase) of the calibration may be determined.

The basic difficulty with this method, however, is that it is difficult to obtain the “standard” EM field environment without having a measurement system that is already calibrated. One way to produce such a standard field is to use a waveguide-like structure for which the internal EM field can be easily calculated from knowledge of the geometry and the input radio-frequency (RF) power being fed into the guide. The double-ended TEM cell is an example of such a wave guiding structure. This device is similar to a coaxial transmission line, with a source at one end and a matched load at another. The source produces a transverse EM (TEM) field within the coaxial line which interacts with the test object located inside the coaxial region, and is ultimately absorbed by the termination impedance.

Figure 13 illustrates a typical double-ended TEM cell, with a cut-away view showing the centre conductor of the coaxial system and the test volume. As long as the test object (i.e., the reference probe to be calibrated) is not too large compared with the cross-section of the cell, the excitation field can be taken to be approximately uniform. Because the TEM mode in this waveguide has no low-frequency cut-off, the calibration may be conducted at very low

frequencies – well below the frequencies permitted by a radiating antenna structure. As the frequency of operation increases, however, other modes and cavity-type resonance can occur and these effectively limit the high frequency utility of the device for calibration purposes. Suppliers of individual TEM cells provide information as to the usable bandwidths of their equipment, which typically range from several tens of kHz to 100 MHz for cells having a working volume on the order of a meter in height. Additional information on TEM cells is provided in IEC 61000-4-20.

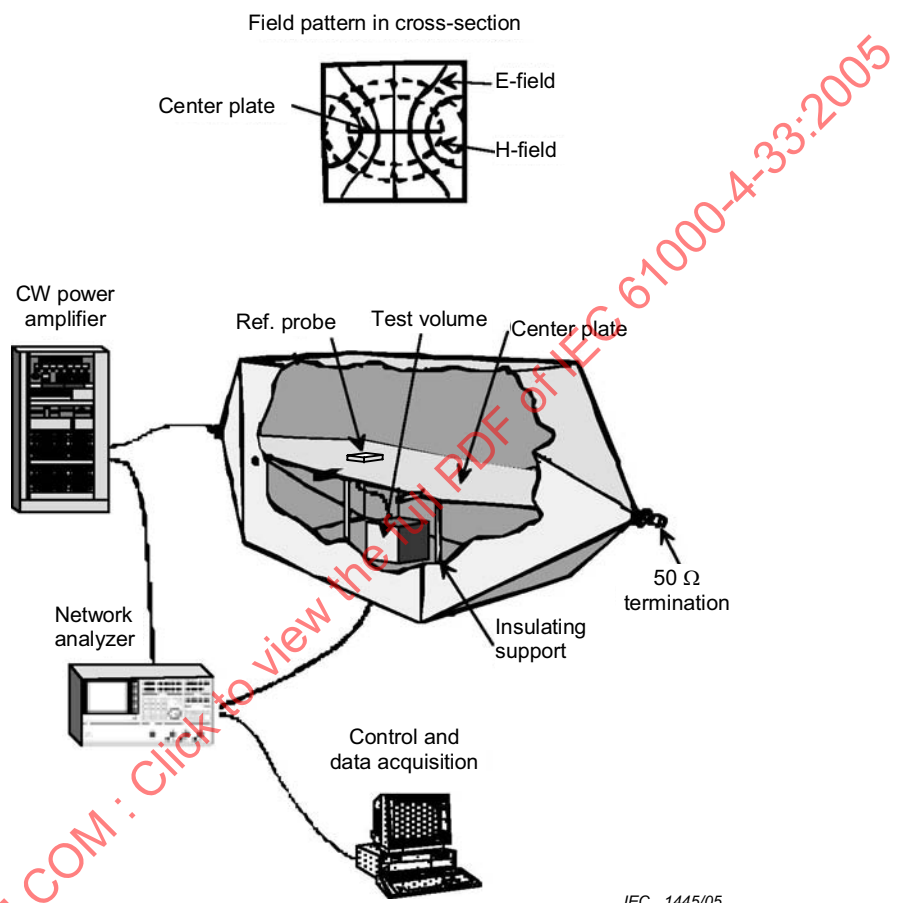


**Figure 13 – The double-ended TEM Cell for providing a uniform field illumination for probe calibration**

An alternative to the double-ended TEM cell described above is the tapered TEM cell as shown in Figure 14. In this test chamber, the inner conductor is offset vertically so as to create a larger test volume, and it has a gradually flared rectangular coaxial cross-section, terminating in a matched load.

The end termination consists of a combination low-frequency circuit element 50- $\Omega$  load, and a high-frequency absorber wall for absorbing the incident propagating wave as in anechoic chambers. The crossover between these two regimes depends on the cell size and the absorber length. The matched broadband impedance load provided by the termination acts to suppress higher modes. The absorbing material significantly increases the losses in the chamber cavity, thereby lowering the resonance effects of the cavity modes. Field uniformity inside the empty chamber can be less than a few dB, for frequencies from DC to 1 GHz (see IEC 61000-4-20).

Cells have been constructed with test chamber heights from 0,5 m to over 3 m for use in testing printed circuit board through box-size equipment. Larger cells capable of complete rack or vehicle testing are under study. The calibration of the measurement chain in these single-ended TEM cells is identical to that discussed for the conventional TEM cell, with the exception that the upper frequency range is higher. Consequently, similar equipment is used (but perhaps with a larger bandwidth).

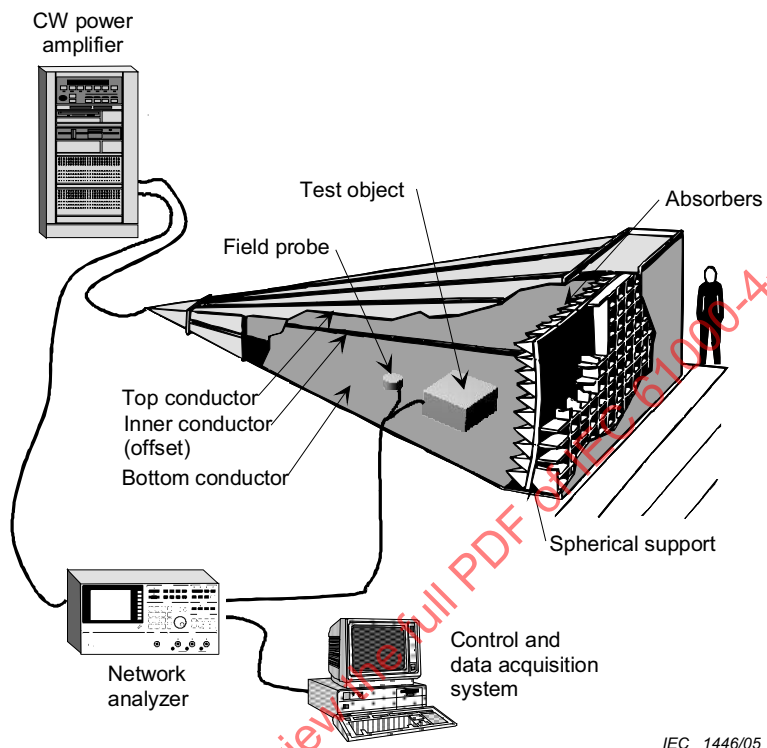


**Figure 14 – Illustration of the single-ended TEM cell and associated equipment**

Such calibration chambers need not be extremely large. For example, Figure 15 shows a small test fixture that has been designed to calibrate single measurement channels from a frequency of about 30 MHz to 1 GHz. Note that while the TEM cell operates well at low frequencies, the 30 MHz limit is due to the poor probe response at low frequencies.

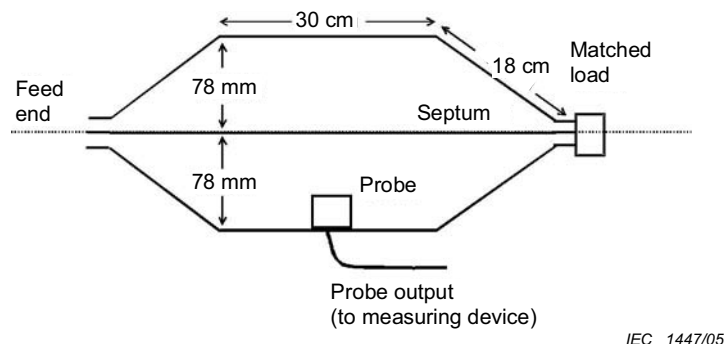


**Figure 15 – Dimensions of a small test fixture for probe calibration**

### 6.1.2 Relative calibration of two measurement channels

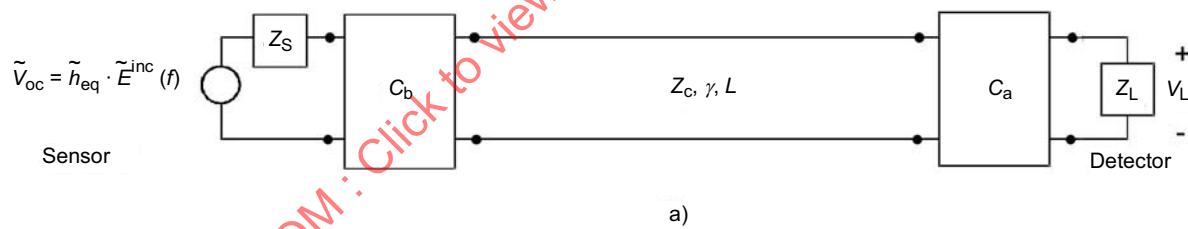
For cases where transfer functions are to be measured, the calibration of the two measurement chains is much simpler, because an accurate knowledge of the excitation EM field environment is not necessary. To perform this calibration, the two sensors of the measurement chains are brought close together so that they measure essentially the same EM field environment, and the ratio of responses is measured. If the two measurement chains are perfectly calibrated, the ratio of these two transfer functions is be unity. However, if one of the chains is uncalibrated, the ratio will differ from unity and this ratio defines the frequency dependent calibration function for this chain.

This calibration process works as long as there are no significant nulls in the spectrum. If a null exists, for example as in the case of E-field excitation at a certain height above the ground where there is a destructive interference from the earth-reflected field, there will be errors in the calibration function. Thus, care must be used in obtaining an excitation field spectrum that is reasonably uniform.

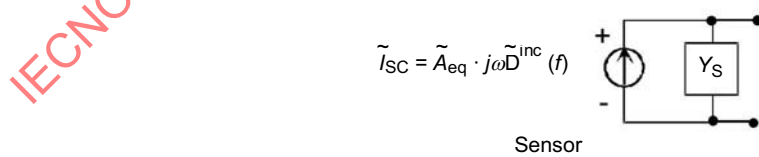
In addition, care shall be taken to ensure that there is minimal mutual interaction between the two measurement sensors when they are brought close together to obtain the calibration factor.

### 6.2 Calibration of individual measurement channel components

An alternate approach to the calibration of a measurement chain is to examine the composition of the chain and to characterize the electrical behaviour of each of its components in such a way that the behaviour of the overall measurement chain can be inferred by combining the data from the components. As an example, the measurement chain illustrated in Figure 1 can be represented electrically by the transmission line network shown in Figure 16.



a)



Sensor

b)

IEC 1448/05

**Figure 16 – Electrical representation of a measurement chain,  
(a) with the E-field sensor represented by a general Thevenin circuit, and  
(b) the Norton equivalent circuit for the same sensor**

### 6.2.1 Representation of the field probe

In the network of Figure 16, the EM field sensor is represented by an open circuit Thevenin voltage  $\tilde{V}_{oc}(f)$ , which is related to the incident E-field through an effective height  $\tilde{h}_{eq}$ , as:

$$\tilde{V}_{oc}(f) = \tilde{h}_{eq} \cdot \tilde{E}^{inc}(f) \quad (13a)$$

together with an input impedance of the sensor,  $\tilde{Z}_s$ . In the most general case, both  $\tilde{h}_{eq}$  and  $\tilde{Z}_s$  are complex-valued, frequency dependent functions, the nature of which depends on the design of the sensor being used.

Alternatively, the sensor may be represented by a Norton equivalent circuit shown in Figure 16b through an equivalent area (or aperture) of the sensor  $\tilde{A}_{eq}$ , the displacement field  $\tilde{D}^{inc} = \varepsilon_0 \tilde{E}^{inc}$  exciting the sensor, and an input admittance  $\tilde{Y}_s = 1/\tilde{Z}_s$ . As discussed by Baum [6], a set of dual expressions are available for magnetic field sensors and the general discussions of the sensor operation here for the E-field sensors will be applicable to the H-field sensors as well. Details of these sensor parameters have been described earlier in 4.3.2.

Considerable confusion arises in testing due to the different ways of defining the calibration factors for measurement probes. When a manufacturer quotes a calibration factor for a probe, it shall be made clear exactly how this factor is defined and how it is to be used in the measurement process.

### 6.2.2 Field probe calibration

When the field sensor is represented as discussed in 6.2.1, the most general calibration procedure amounts to determining the two complex-valued functions — the equivalent height and the input impedance — as a function of frequency over the band of interest. If the sensor is loaded internally or its behaviour when loaded by a known, fixed impedance is desired, then only a knowledge of the loaded voltage response is needed, which is given in terms of the modified equivalent height  $\tilde{h}_{eq}$ .

Determining these quantities can be done either experimentally or analytically, as outlined below.

#### 6.2.2.1 Probe calibration by ruler

In some cases, it is possible to obtain the calibrating factors of a field probe using analytical methods [5]. For certain shapes of conductors (like a sphere or a spheroid for example), it is possible to derive an analytical expression for the open-circuit voltage and the input impedance by solving a classical scattering problem. Although these solutions can be rather complicated and have a strong frequency variation, if one assumes that the sensor is electrically small, it can be demonstrated that the sensor voltage can be specified as in equation (13), with the  $\tilde{h}_{eq}$  parameter being given by a closed-form expression. This has been referred to as “calibration by the ruler” because all that is needed to determine the sensor’s sensitivity, in principle, is a measurement of its dimensions, (plus, of course, the analytical expressions giving the response).

Such calibration by the ruler is useful due to its simplicity, but there can be several disadvantages in relying on this technique. These are:

- only a limited number of sensors may be analytically calibrated by this manner;
- the frequency range of the calibration validity is limited by the sensor size and no provision for exceeding the maximum frequency of operation is available; and
- this calibration procedure does not take into account possible manufacturing flaws and imperfections which may cause the sensor to have a non-ideal response.

For sensors that cannot be calibrated by such analytical means, it is possible to measure the pertinent calibration factors at low frequencies. As long as the low-frequency limitations are observed, such sensors can be described by the two scalar coefficients that may be measured at any frequency within the operational bandwidth.

#### 6.2.2.2 Sensor calibration by substitution

An alternative calibration method for sensor calibration is to compare its response in an unknown EM field environment with that of another, previously calibrated sensor [5]. This process results in what is often referred to as a calibration *traceable* to some accepted standard. In doing this type of calibration, it is important to maintain the reference sensor in a clean and undisturbed physical condition, as any error in its response can lead to errors in the calibration function.

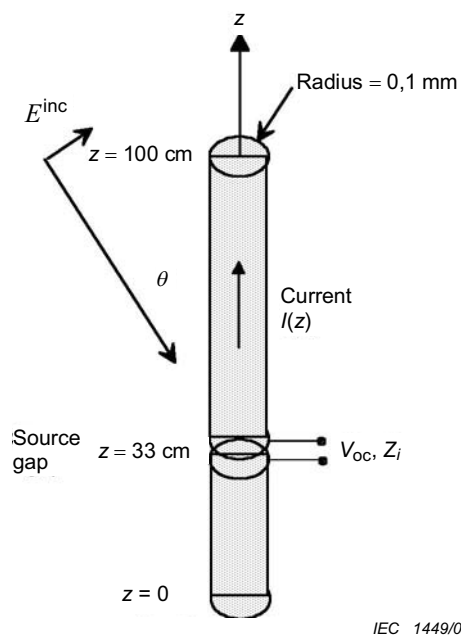
#### 6.2.2.3 Probe calibration by analysis

In some cases, it is possible to calibrate a field probe by performing an accurate EM coupling analysis. Typically, such an analysis involves solving an integral equation for the induced charge and current on the sensor that are produced by the incident EM field [7]. Several computer programs are available for this analysis.

Notwithstanding the recent developments made in numerical modelling in the past few years, only relatively simple sensor shapes can be considered. Moreover, it is often difficult to model the details of the feeding structure for such sensors without an undue amount of effort. Nevertheless, this approach for calibration can be fruitful in some cases.

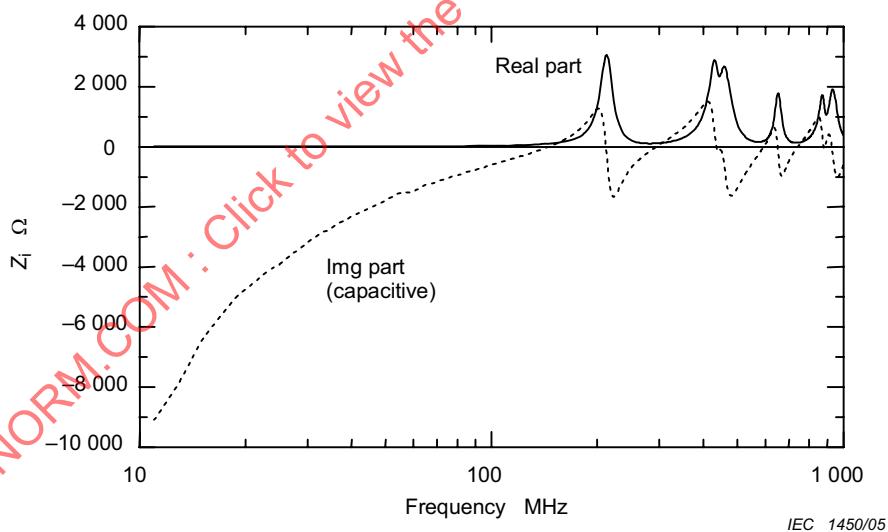
As an example of this procedure, Figure 17 illustrates a very simple E-field probe: a cylindrical conductor of length  $L = 1$  m and radius  $a = 0,1$  mm. Its feed point is located at a distance  $z = 33$  cm from one end (an offset feeding point has been used to make the results more interesting), and an incident E-field is assumed to be incident at an angle  $\theta$  with respect to the cylinder axis.

As noted in 6.2.1, the input impedance of this probe at its terminals is one of the required parameters for characterizing the device. By placing a unit voltage source across the input terminals, an antenna analysis code can be used to compute the induced current flowing on the conducting surface. From a knowledge of the current flowing just at the sensor terminals, denoted by  $\tilde{I}_i$ , the input admittance is obtained as  $\tilde{Y}_i = \tilde{I}_i$ , and the input impedance is the inverse,  $\tilde{Z}_i = 1/\tilde{I}_i$ .



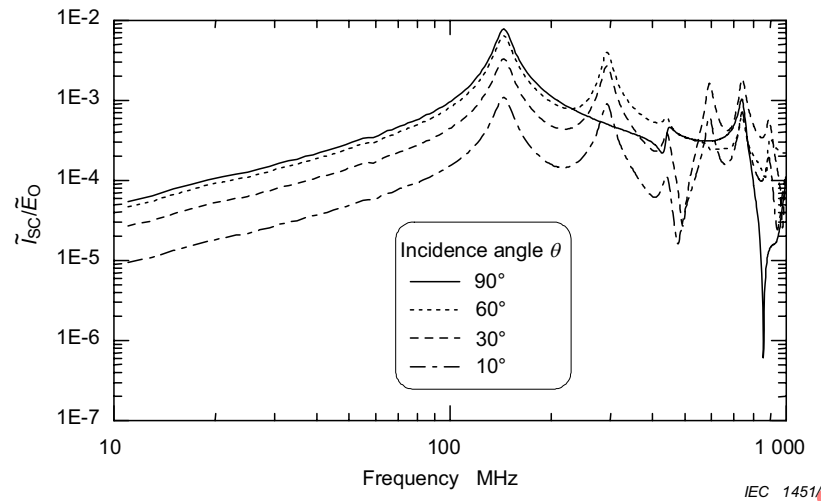
**Figure 17 – Example of a simple E-field probe**

Figure 18 presents a plot of the real and imaginary parts of the input impedance,  $Z_i$ , of the sensor as a function of frequency. Note that for frequencies below about 100 MHz the impedance is basically capacitive, with a value of capacitance of  $C \approx 1,7 \text{ pF}$ . Also notice that the real part of the impedance is always positive – a requirement from energy conservation concepts.



**Figure 18 – Plot of the real and imaginary parts of the input impedance,  $Z_i$ , for the E-field sensor of Figure 17**

The antenna analysis code can also be used for computing the response of the sensor to an incident field. For an E-field incident at an angle  $\theta$  as illustrated in Figure 17, Figure 19 presents the magnitude of the induced short-circuit current flowing into the terminals of the sensor as a function of frequency and for different angles of incidence. Note that below 100 MHz, the response is rather smooth, with the various sensor resonances occurring first at 150 MHz and at the higher harmonics. It is in the smooth frequency range that the sensor is designed to operate efficiently.



**Figure 19 – Plot of the magnitude of the short-circuit current flowing in the sensor input for different angles of incidence, as computed by an antenna analysis code**

By performing a Norton to Thevenin transformation, the open-circuit voltage of the sensor can be determined. This type of sensor responds to the E-field tangential to the wire axis, which is given by  $\tilde{E}^{inc}(f)\sin(\theta)$ , and in this case, it is desirable to compute an effective height that is a function of the incidence angle, as

$$\tilde{h}_{eq}(\theta) = \frac{\tilde{V}_{oc}(f)}{\tilde{E}^{inc}\sin\theta} . \quad (13b)$$

Figure 20 illustrates the resulting plots for this equivalent height of the sensor. At low frequencies, we note that the antenna responds proportionally to the tangential E-field along the length of the cylinder, with an equivalent height of  $\tilde{h}_{eq} = 0,5$  m. At higher frequencies, however, we note that the various sensor resonances disturb this calibration factor and that a general complex-valued function must be used. Moreover, the degree of variation in the calibration factor depends on the angle of incidence, thus implying that different calibration factors are required for different angles of incidence. Nevertheless, if the sensor's operation is limited to the low frequency regime (<100 MHz in this case), a simple capacitance and equivalent height is sufficient to characterize the sensor.

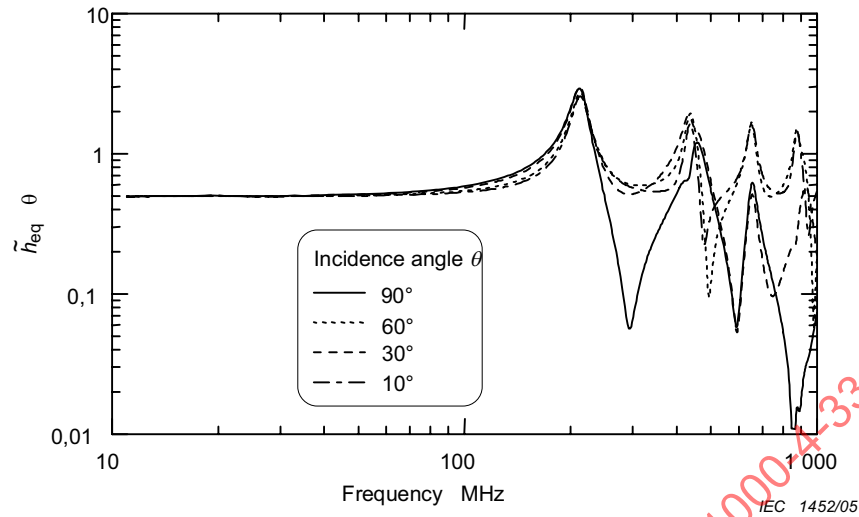


**Figure 20 – Plot of the magnitude of the effective height of the sensor for different angles of incidence**

#### 6.2.2.4 Probe calibration by measurement in a standard EM environment

An alternative to the analytical calibration procedure in the preceding clause involves the direct measurement of the sensor output in a known EM environment. As discussed in Clause 6.1.1, the main difficulty with this approach is knowing the EM environment in the first place. Typical test procedures will involve placing the sensor in a test chamber or other well-controlled environment and then making a measurement of the sensor output as a function of frequency. This response is normalized by the incident field strength to provide a transfer function of the sensor (in both magnitude and phase) as a function of the frequency of the EM field. As discussed above, if the sensor is unloaded, the response will be reasonably constant (i.e., flat) in the bandwidth of operation. If the sensor is loaded internally, the response will be observed to grow proportionally to the frequency  $\omega$ .

In addition to the voltage response calibration of the sensor, the input impedance is needed. For an unloaded E-field sensor, this impedance will be primarily a capacitance (or an inductance for a H-field sensor). At higher frequencies, parasitic elements within the sensor can become important and a measurement of these effects is required.

In measuring both of these sensor parameters, it is important to take into consideration the dynamic range limitations of the measuring equipment. Such measurements are always limited by the “noise floor” of the test equipment, and this limits the accuracy of the measurements. Moreover, when measuring large transient signals, the presence of possible nonlinear effects in the sensors can invalidate these linear calibration functions.

#### 6.2.3 Construction of the calibrated measurement chain from individual components

Once the individual probes are represented by an equivalent circuit and suitably calibrated using one of the methods described in the preceding clause, the overall measurement chain can be calibrated by representing the various elements in terms of one of the two-port models described in Annex D or if a matched system one can use equation (5).

Using the scattering (S) parameters, which are most easily measured using a network analyser, the calibration of the measurement channel shall be conducted as follows.

- a) Remove each of the two-port devices (the attenuator, cable, balun, etc.) from the measurement chain.
- b) Measure the S-parameters of the two-ports in accordance with the procedure given by the network analyser manual.
- c) Convert the S-parameters into the chain parameters using equation (D.18).
- d) Multiply all of the chain parameter matrices for the measurement channel components together, as indicated in equation (D.8), to find the total chain parameter representation for the channel.
- e) With the specification of the sensor as a Thevenin equivalent circuit, use equation (D.10) to evaluate the load response voltage  $\tilde{V}_L$ .
- f) Compute the overall calibration function for the measurement chain as  $\tilde{K}(f) = \tilde{V}_L(f) / \tilde{E}^{\text{inc}}(f)$ , where  $K(f)$  is a variable describing the calibration function.

### 6.3 Approximate calibration techniques

In the absence of accurate calibration data for a measurement chain, there are several approximate ways of obtaining the necessary data for using the measuring system. These approaches can be designed to provide either the simple scalar coefficients of the measurement chain elements described in 4.3.1, or they can provide estimates of the complex-valued, frequency dependent responses of the elements. These approximate calibration techniques shall be considered as a method of last resort, as an accurate calibration of the elements is always preferable.

In this clause, we will discuss some of the various methods for obtaining approximate calibration functions.

#### 6.3.1 Scalar calibration of the overall measurement chain

The simplest method for obtaining an approximate calibration factor for the overall measurement chain is to assume a frequency-independent attenuation function for each of the components in the system and apply these to reduce the response at the measurement location. The representation of the measurement chain in this manner has been described in 4.3.1.

In this calibration approach, the goal is to determine the scalar factor  $K$  in equation (9), which permits the determination of the excitation field from the measured response of the measurement chain. This can be accomplished either by determining the individual scalar factors  $K_i$  that are multiplied together to provide the overall factor  $K$ , or by calibrating the overall measurement chain directly. This latter calibration can be performed using the substitution method (see 6.2.2.2) by making a measurement of the excitation field with a previously calibrated sensor (and associated equipment) and then relating this known field strength to the measurement made with the system being calibrated.

#### 6.3.2 Circuit modelling

A more accurate method for determining the calibration of the measurement system is to use the chain parameter solution for the load voltage response in terms of the open circuit voltage of the sensor, which is related to the incident field through the sensor calibration factor. This expression is given in equation (D.10) in Annex D. To determine the various elements in the overall chain parameter matrix, a simple, frequency-dependent circuit model for each component of the measurement chain can be developed, and the results combined using equation (D.8).

### 6.3.2.1 Transmission line model

For example, the chain parameter representation for the transmission line section is given in equation (D.12) of Annex D, and involves the characteristic impedance and propagation constant of the line. Generally, these parameters are functions of frequency. Assuming that a typical transmission line can be characterized by a per-unit-length inductance  $L'$ , capacitance  $C'$ , resistance  $R'$  and conductance  $G'$ , the general expressions for the complex-valued propagation constant  $\gamma$  and the characteristic impedance are [7]

$$\gamma = \sqrt{(R' + j\omega L')(G' + j\omega C')} \text{ and } Z_c = \sqrt{\frac{(R' + j\omega L')}{(G' + j\omega C')}}. \quad (14)$$

Usually, such lines in practical measurement systems are low loss, implying that  $R' \ll \omega L'$  and  $G' \ll \omega C'$ . Under these assumptions, the propagation constant becomes

$$\gamma \approx \frac{1}{2} \left( \frac{R'}{Z_c} + G' Z_c \right) + j\omega \sqrt{L' C'} \quad (15)$$

and the characteristic impedance  $Z_c$  is

$$Z_c \approx \sqrt{\frac{L'}{C'}}. \quad (16)$$

Using these parameters in equation (D.12) will provide a frequency-dependent model for the transmission line section.

### 6.3.2.2 Attenuator model

Similar modelling can be developed for the other two-port elements of the measurement chain. One common element is a simple attenuator, which is to be inserted into the transmission line having a characteristic impedance of  $Z_c$  and to provide an attenuation factor  $\alpha$ .

A simple model of the attenuator at dc is given by the Tee circuit shown in Figure 4. If it is assumed that the attenuator is operating in a  $50\Omega$  transmission system, the values of the resistive elements  $R_1$  and  $R_2$  can be shown to have the following values for a specified attenuation factor  $\alpha$ :

$$R_1 = 50 \frac{1-\alpha}{1+\alpha} \text{ and } R_2 = 100 \frac{\alpha}{(1+\alpha)(1-\alpha)}. \quad (17)$$

Combining the three elements of the attenuator together in a manner similar to what was done for equation (D.11) of Annex D permits the development of the overall chain parameter matrix for the two-port attenuator. This becomes

$$[C] = \begin{bmatrix} 1 & R_1 \\ 0 & 1 \end{bmatrix} \begin{bmatrix} 1 & 0 \\ R_2 & 1 \end{bmatrix} \begin{bmatrix} 1 & R_1 \\ 0 & 1 \end{bmatrix} \quad (18)$$

$$= \begin{bmatrix} \frac{1}{2} \left( \frac{\alpha^2 + 1}{\alpha} \right) & \frac{25}{\alpha} (1 - \alpha^2) \\ \frac{1}{100\alpha} (1 - \alpha^2) & \frac{1}{2} \left( \frac{\alpha^2 + 1}{\alpha} \right) \end{bmatrix},$$

which is an expression for the chain parameters in terms of the attenuation factor  $\alpha$  of the circuit.

This model can be extended to higher frequencies by including the effects of parasitic capacitances at the input and output terminals of the circuit, as shown in Figure 21. This circuit can be analysed as before by adding the individual contributions of the capacitances to the chain parameters. In addition, the effects of lead inductances may be included in the same manner.

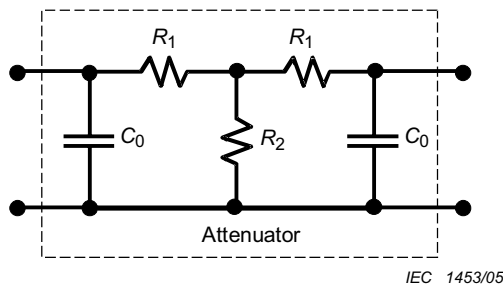


**Figure 21 – High frequency equivalent circuit of an attenuator element**

### 6.3.3 Fitting functional approximation of calibration functions

At times, calibration curves of the response of a circuit or network component may be provided in lieu of an accurate circuit model or digitised data. Frequently, such data are in the form of magnitude-only responses. Using a graphical approach known as the Bode diagram, it is possible to examine the responses on a log-log plot and infer a rational polynomial approximation for the function. This is done by identifying the asymptotes of the spectral curve, finding their slopes on the log-log plot (which must be integer values) and identifying the crossing frequencies of the asymptotes. Details of this approach are discussed in more depth in [8].

## Annex A (normative)

### Methods of characterizing measured responses

#### A.1 Waveform parameters

For the HEMP environments, IEC 61000-2-9 and IEC 61000-2-10 describe the important features of the incident E- and H-fields that can excite a system, or the conducted transients that can flow on cables attached to equipment. Similarly, for the HPEM environments there are both incident field and conducted transients that must be defined.

Of the many different waveforms encountered in EM testing, there are several that appear regularly in such measurements. The first common waveform class appears like a single pulse function, as shown in Figure A.1. This main portion of the waveform consists of a rapidly rising and falling monopolar pulse, which can be characterized by the rise time, pulse width, maximum rate of rise, and peak value. Not shown in this figure are low-level pre-pulse and late-time waveform components, which may occur in some waveforms. If this type of waveform is used to describe a radiated transient EM field in the far-zone, then there is a requirement that the integrated area under the waveform curve of Figure A.1 must be zero. Thus, for this case the pre-pulse and late time waveform components are important, as they must cancel out the area under the primary pulse shown in this figure.

The waveform parameters used to characterize the main peak of the waveform in Figure A.1 include the following parameters for a transient response  $R(t)$ :

- The peak value  $R_{\max}$ ,
- The time to the peak value,  $t_{\text{peak}}$ ,
- The 10-90 % rise time,  $\Delta t_{10-90}$ ,
- The pulse width, defined as the “full-width at half max” (FWHM), which is the difference in time between the initial 50 % peak value point in the waveform and the late-time point in the waveform having the same value,  $\Delta t_{50-50}$ ,
- The maximum rate of rise =  $(dR/dt)_{\max}$  for  $t < t_{\text{peak}}$  .

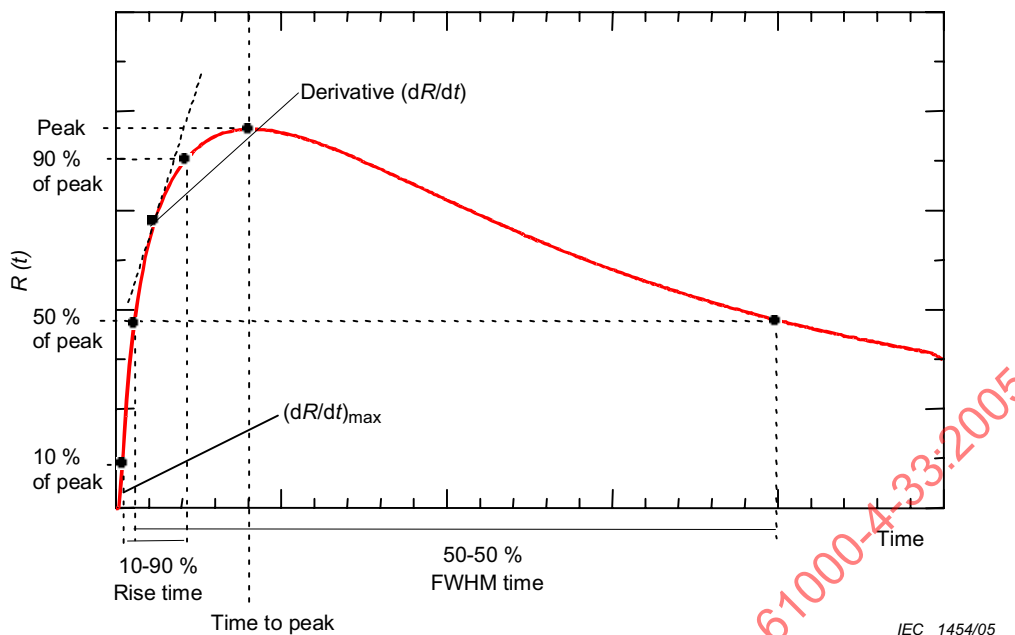


**Figure A.1 – Illustration of various parameters used to characterize the pulse component of a transient response waveform  $R(t)$**

In addition to the single pulse response shown in Figure A.1, high-power transient measurements often result in oscillatory waveforms similar to that shown in Figure A.2. The waveform parameters illustrated in Figure A.1 can also be used in this case to characterize the primary peak of the response. However, there are two additional parameters that are needed to describe this waveform. They are the  $1/e$  fall time  $t_f$  of the envelope of the oscillations (which can be related to a quality factor of the waveform), and  $T$ , the average period of the oscillations. These parameters, together with the pre-pulse and noise contributions are illustrated in Figure A.2.

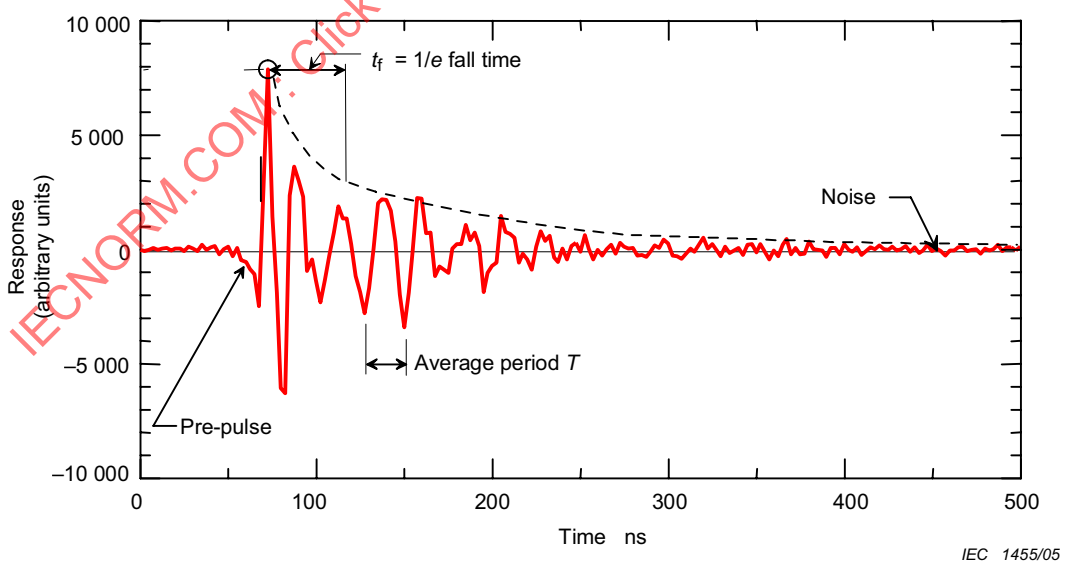


**Figure A.2 – Illustration of an oscillatory waveform frequently encountered in high-power transient EM measurements**

## A.2 Waveform norms

Another type of waveform parameter is the time waveform p-norm  $\|R\|_p$ , as defined in reference [A.1] as

$$\|R\|_p = \left\{ \int_{-\infty}^{\infty} |R(t)|^p dt \right\}^{1/p}, \quad (A.1)$$

where  $p$  is an integer: 1, 2, etc. Note that these norm quantities generally involve a mathematical operation on the entire waveform through the integration process, as opposed to the simple waveform parameters of Clause A.1.

NOTE The infinity norm ( $p = \infty$ ) is an exception, in that although it does involve the integration process, its result can be obtained from a simple examination of the waveform.

Table A.1 illustrates three commonly used waveform norms for high-power response characterizations.

**Table A.1 – Examples of time waveform p-norms**

Value of $p$	Waveform Norm Attribute	Physical Quantity
1	$\int_{-\infty}^{\infty}  R(t)  dt$	Rectified impulse value of response
2	$\left\{ \int_{-\infty}^{\infty}  R(t) ^2 dt \right\}^{1/2}$	Square root of the action integral response
$\infty$	$ R(t) _{\max}$	Peak value of response

The norms used in Table A.1 are commonly used in the characterization of high-power EM responses. Table A.2 provides a tabulation of the norms  $N_1$  –  $N_5$ , which are typically used for waveform characterisation, together with an indication as to why the norm is of particular interest.

**Table A.2 – Time waveform norms used for high-power transient waveforms**

p-Norm	Norm Quantity	Name	Example of use
$\ R\ _{\infty}$	$N_1 =  R(t) _{\max}$	Peak (absolute) value	Circuit upset
n/a	$N_2 =  \partial R(t) / \partial t _{\max}$	Peak (absolute) value of the rate of rise	Component arcing; circuit upset
n/a	$N_3 = \left  \int_0^t R(x) dx \right _{\max}$	Peak (absolute) impulse	Dielectric puncture (if R denotes the E-field)
$\ R\ _1$	$N_4 = \int_0^{\infty}  R(x)  dx$	Rectified total impulse	Equipment damage
$\ R\ _2$	$N_5 = \left\{ \int_0^{\infty}  R(x) ^2 dx \right\}^{1/2}$	Square root of action integral	Component burnout

### A.3 Waveform spectrum

Another waveform attribute that is useful is its frequency spectrum,  $\tilde{R}(f)$ . This is a complex-valued function of the frequency  $f$ , and for an infinitely long, continuous transient response  $R(t)$ , it is defined by the Fourier transform integral as defined in reference [A.2]

$$\tilde{R}(f) = \int_{-\infty}^{\infty} R(t) e^{-j2\pi ft} dt. \quad (\text{A.2})$$

NOTE Note that reference [A.2] uses the notation  $\exp(-j\omega t)$  for time harmonic signals, whereas in this document we use the conventional engineering notation  $\exp(j\omega t)$ .

Usually, for a measured transient response, the function  $R(t)$  is not known for all times, but rather, it is a sampled function of  $N$  values at discrete time points  $t_i$  which are uniformly spaced between  $t = 0$  and  $t = T_{\max}$ . This results in a time difference between samples of  $\Delta t = T_{\max}/(N-1)$ , and the implication of this is that the frequency spectrum is periodic in frequency, with the principal spectrum being defined within the Nyquist frequency limits of  $\pm F_{\max} = 1/(2\Delta t)$ . Outside this frequency range, the spectrum repeats itself. Thus, if the response waveform is band-limited (e.g., if it has no significant frequency components above a maximum frequency  $F_{\max}$ ), it can be adequately represented by the discrete time samples. This is known as the sampling theorem.

Moreover, in numerically evaluating equation (A.2), the responses also will be evaluated at discrete frequency points  $f_k$ , and a simple approximation to the integral is

$$\tilde{R}(f_k) \approx \Delta t \sum_{i=0}^{N-1} R(t_i) e^{-j2\pi f_k t_i}. \quad (\text{A.3})$$

Usually in the evaluation of the discrete Fourier transform in equation (A3), the frequency points are chosen to be  $f_k = k/(N\Delta t)$  for  $k = -N/2, \dots, N/2$ . Notice that the sampling interval in the frequency spectrum,  $\Delta f = 1/(N\Delta t) = 1/T_{\max}$ . Thus, the length of the transient record has a direct impact on the low-frequency resolution of the spectrum.

This discrete nature of the frequency spectrum implies that the transient response is also a periodic function of time. The discrete spectrum  $\tilde{R}(f_k)$  can be evaluated either by a direct evaluation of the sum or by the use of the Fast Fourier transform, which is a much more rapid way of calculating the spectrum. Details are provided in reference [A.2].

The fact that both the transient response and its frequency domain spectrum are periodic functions with period  $T_{\max}$  and  $F_{\max}$ , respectively, means that care must be used to avoid the occurrence of aliasing – both in the time domain and in the frequency domain. Aliasing occurs when there is a “feed-through” of the response or the spectrum from one period to another, thereby contaminating the results. Thus, all calculated transient and spectral responses must be carefully examined to be certain that aliasing is not a problem.

As an example of the frequency spectrum of a transient response, Figure A.3 shows the magnitude of the spectrum of the oscillatory waveform of Figure A.2. The corresponding phase is not shown in this plot.

The actual time domain waveform of Figure A.2 consists of  $N = 1\,024$  points and runs to a total time of  $T_{\max} = 2,555 \mu\text{s}$  (although the plot only shows the first 500 ns of the waveform). This means that the time sampling is  $\Delta t = T_{\max}/(N-1) = 2,497 \text{ ns}$ . Consequently, for the waveform in Figure A.2 the Nyquist frequency is  $F_{\max} = 1/(2\Delta t) = 200 \text{ MHz}$ , and the spectrum sampling interval is  $\Delta f = 1/T_{\max} = 0,391 \text{ MHz}$ .

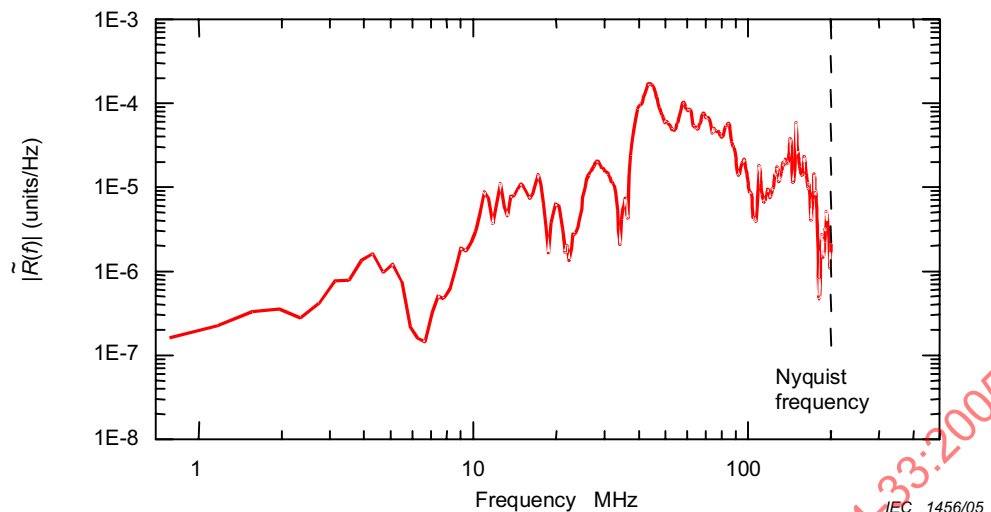


**Figure A.3 – Example of the calculated spectral magnitude of the waveform of Figure A.2**

#### A.4 References

- A.1 BAUM, CE. Norms and Eigenvector Norms. *Mathematics Notes*, Note 63, Kirtland AFB, New Mexico, November 1979.
- A.2 PRESS, WH., et. al. *Numerical Recipes*, Cambridge University Press, Cambridge, 1986.

## Annex B (informative)

### Characteristics of measurement sensors

#### B.1 Free-field electric field sensors

Sensors that are designed to measure the E-field are basically antennas that operate well below their first resonant frequency. At low frequencies, the response of the antenna is approximately proportional to the frequency, and consequently, the behaviour of the antenna can be characterized rather simply.

Figure B.1 illustrates a generic E-field sensor, which is connected to a load element representing the measurement chain equipment. This sensor is often called a “free-field” sensor, as it is designed to operate well away from any objects that can perturb the local E-field. The sensor is represented by a Norton equivalent circuit, as shown in the right part of Figure B.1.

**NOTE** Of course, the equivalent Thevenin circuit could be used to represent this E-field sensor as well. This results in the sensor being described in terms of its open circuit voltage, which is related to the excitation E-field by an equivalent height of the antenna. Most sensor manufacturers, however, tend to characterize their sensors in terms of the equivalent area, and consequently, the Norton equivalent is preferred. For more details, consult Baum, C. E., “Electromagnetic Topology for the Analysis and Design of Complex Electromagnetic Systems”, pp. 467-547 in *Fast Electrical and Optical Measurements*, Vol. I, Eds. I.E. Thompson and L.H. Luessen, Martinus Nijhoff, Dordrecht, 1986, page 77.

The short-circuit current source for this sensor can be thought of as arising from the time variation of the charge induced on the metal elements of the sensor by the local excitation E-field. This is conveniently expressed in the time domain using an equivalent area of the sensor,  $A_{eq}$ , as

$$I_{sc}(t) = \frac{\partial Q(t)}{\partial t} = -A_{eq} \frac{\partial}{\partial t} (\hat{z} \cdot \vec{D}_o(t)), \quad (B.1)$$

where  $\vec{D}_o(t) = \epsilon_0 \vec{E}_o(t)$  is the electric displacement field, and  $\epsilon_0 = 8,854 \times 10^{-12}$  (F/m) is the permittivity of free space.

In the frequency domain, where  $f$  denotes the frequency and  $\omega = 2\pi f$  is the angular frequency, this expression for the Norton current source term is

$$\tilde{I}_{sc}(\omega) = j\omega \tilde{Q}(\omega) = -A_{eq} j\omega \left( \hat{z} \cdot \tilde{\vec{D}}_o(\omega) \right). \quad (B.2)$$

At low frequencies when the antenna is electrically small, the sensor impedance can be approximated by a capacitance, because the real part of the sensor impedance (the radiation resistance) is negligible. As the frequency approaches the resonant frequency of the probe, a single capacitance is no longer a suitable approximation, and a more complicated sensor impedance representation is needed.

The load resistance,  $R$ , represents the load placed on the sensor by the measurement chain. Usually the measurement chain uses a 50-Ω coaxial cable to link components. Because the E-field sensor has a balanced output, it is necessary to have a balun to convert this balanced output to an unbalanced 50-Ω coaxial line. Such a balun changes the impedance level of the lines, and as a consequence, the effective resistance that loads the sensor is typically 100 Ω. More information on the balun element is provided in 4.3.3.

In addition to the measurement equipment resistance  $R$ , another resistance  $R_o$  may be located in series with the equipment. This resistance is not present in all E-field sensors, and as will be discussed shortly, this resistance can be used to adjust the operation of the sensor.

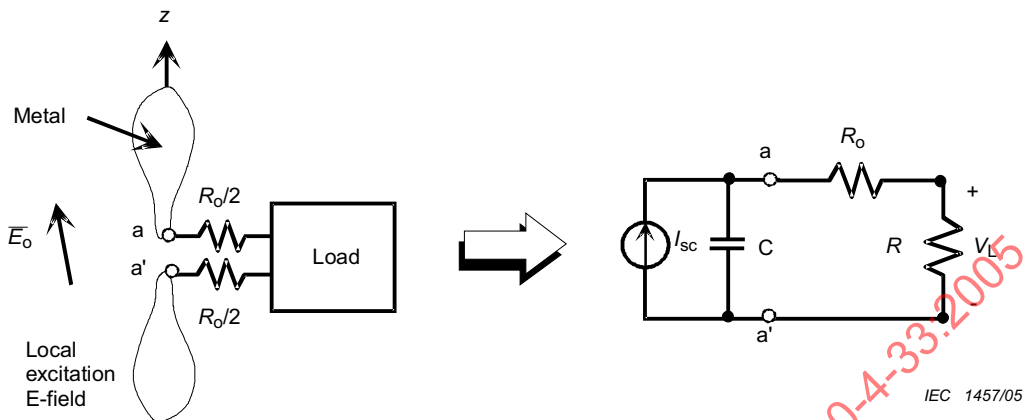


**Figure B.1 – Illustration of a simple E-field sensor, together with its Norton equivalent circuit**

A simple frequency domain analysis of the Norton circuit provides the following response for the voltage across the load

$$\begin{aligned}\tilde{V}_L(\omega) &= \frac{\tilde{I}_{sc}R}{1+j\omega C(R+R_o)} \\ &= \frac{-j\omega A_{eq}R\varepsilon_o \tilde{E}_{oz}(\omega)}{1+j\omega C(R+R_o)}\end{aligned}\quad (B.3)$$

where  $\tilde{E}_{oz}$  denotes the z-component of the external E-field in the frequency domain. By defining the normalized frequency function  $\tilde{F}(\omega\tau)$  as

$$\tilde{F}(\omega\tau) = \frac{j\omega\tau}{1+j\omega\tau}, \quad (B.4)$$

the general expression for the load voltage of the E-field sensor in equation (B.3) becomes

$$\tilde{V}_L(\omega) = -\frac{A_{eq}\varepsilon_o}{C} \frac{R}{(R+R_o)} \tilde{F}(\omega\tau_{RC}) \tilde{E}_{oz}(\omega) \quad (\text{where } \tau_{RC} = (R+R_o)C), \quad (B.5)$$

or equivalently,

$$\tilde{V}_L(\omega) = \tilde{T}_{\text{sensor}}(f) \tilde{E}_{oz}(f). \quad (B.6)$$

This last equation defines the frequency domain transfer function  $\tilde{T}_{\text{sensor}}(f)$  used to represent the E-field sensor in the overall measurement chain. Frequently, the quantity  $\tilde{T}_{\text{sensor}}$  is referred to the equivalent height of the sensor, and is denoted as  $h_e(f)$ .

The function  $F$  of equation (B.4) provides the frequency dependence of the sensor operation and it is plotted in Figure B.2. Both the magnitude and phase of this function are shown. At sufficiently low frequencies, where  $\omega\tau \ll 1$ , the frequency function is approximately  $j\omega$ , which indicates that the sensor response is proportional to the rate of rise of the E-field. For high frequencies, where  $\omega\tau \gg 1$ , the frequency function is a constant, indicating that the sensor response is proportional to the E-field. In between these two regions is the transition region where the response smoothly changes from one behaviour to another. These regions are indicated in Figure B.2.

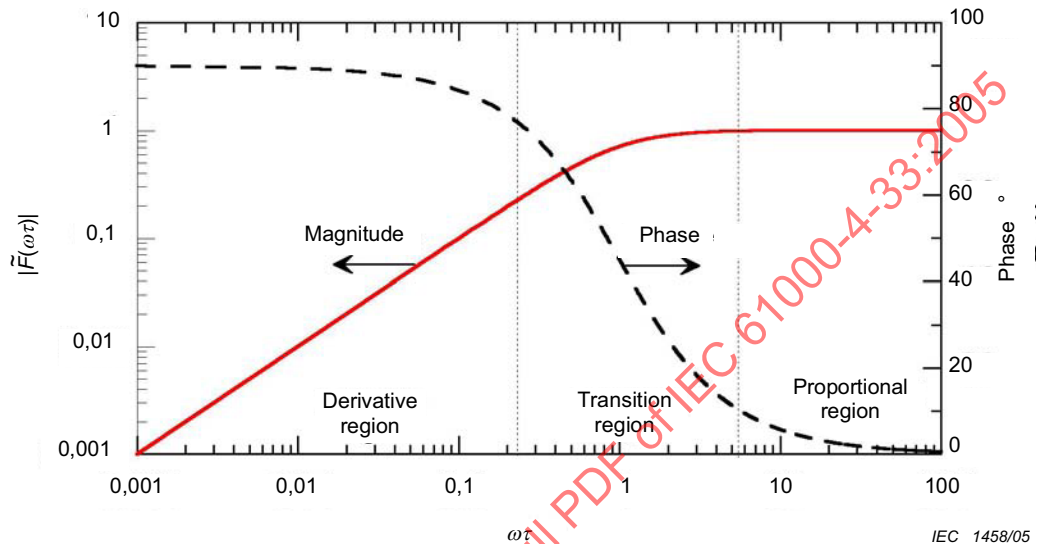


**Figure B.2 – Magnitude and phase of the normalized frequency function  $\tilde{F}(\omega\tau)$  for the field sensor**

### B.1.1 Derivative (D-dot) sensors

By selecting a proper design of the sensor parameters, it is possible to construct a sensor that responds to the rate of rise of the excitation E-field. For example, if the RC time constant  $\tau_{RC} = (R+R_o)C$  in equation (B.5) is chosen to be very small, the response will be proportional to  $j\omega$ , and hence, the sensor will operate as a differentiating device. This can be done by omitting the resistance  $R_o$ , and requiring that  $1/\tau_{RC} = 1/(RC) \gg 2\pi f_{\max}$  where  $f_{\max}$  is the maximum frequency in the spectrum for which the sensor is to be used.

Under these assumptions, the load voltage of equation (B.5) is

$$\tilde{V}_L(\omega) \approx -j\omega A_{eq} R \varepsilon_o \tilde{E}_{oz}(\omega) \quad (R_o = 0; 2\pi f \ll 1/RC). \quad (B.7)$$

In the time domain, this expression for the load voltage is

$$V_L(t) \approx -A_{eq} R \varepsilon_o \frac{\partial}{\partial t} (E_{oz}(t)) , \quad (B.8)$$

which is valid as long as the rise time  $t_r$  of the measured E-field is  $t_r \ll RC$ .

Such sensors are referred to as D-dot sensors, since their response is proportional to the rate of rise (e.g., the derivative) of the electric displacement vector,  $D$  (or to the electric field,  $E$ ). Sensor manufacturers will usually specify such sensors by the equivalent area,  $A_{eq}$ , and by the upper cut-off frequency  $f_{max} = 1/(2\pi RC)$ , rather than by the intrinsic capacitance and resistance of the sensor. In this manner, the manufacturer assumes that such sensors will always be operated with an effective load resistance of  $100 \Omega$ . If such sensors are used with other loads, or in frequency regimes where the simple  $j\omega$  response is not possible, one must use the more general calibration function of equation (B.5) to obtain the E-field from the measured sensor voltage.

When the E-field sensor is used in the derivative mode (e.g., when it is measuring the rate of rise of the E-field), it is necessary to integrate its response to determine the actual value of the E-field. As noted in Figure 1 of this standard, this can be done by inserting an integration device in the measurement chain, or it can be done numerically in a post-processing of the data.

### B.1.2 Direct E-field sensors

By changing the parameters of the E-field sensor, it is possible to develop a sensor that responds directly to the excitation field, rather than to its rate of rise (temporal derivative). By selecting the  $RC$  time constant in equation (B.5) such that  $1/\tau_{RC} = 1/(R+R_o)C \ll 2\pi f_{min}$  where  $f_{min}$  is the minimum frequency of the spectrum to be measured, the load voltage becomes

$$\tilde{V}_L(\omega) = -\frac{A_{eq}\epsilon_0}{C} \frac{R}{(R+R_o)} \tilde{E}_{oz}(\omega) \quad (2\pi \gg 1/(R+R_o)C) \quad . \quad (B.9)$$

Note that because  $R$  is fixed at a nominal value of  $100 \Omega$ , to satisfy the requirement that  $1/(R+R_o)C \ll 2\pi f_{min}$ , we can either increase the series resistance  $R_o$ , or increase the capacitance  $C$ . Doing either will decrease the sensitivity of the sensor, as noted in equation (B.5).

In the design of such direct response sensors, the resistance element is often the one that is changed. Given a fixed size for the sensor elements, different resistance values for  $R_o$  can be provided to tune the bandwidth of the sensor.

## B.2 Free-field magnetic field sensors

The free-field magnetic field sensor shown in Figure B.3 is the electrical dual to the E-field sensor. A time varying magnetic flux ( $\Phi$ ) passing through the loop will induce a voltage in the load resistance, which will be measured. For sufficiently slow transient excitation fields (such that their rise times are much longer than the transit time across the loop), the open circuit Thevenin voltage source of the loop is given as

$$V_{oc}(t) = \frac{\partial \Phi(t)}{\partial t} = A_{eq} \frac{\partial}{\partial t} (\hat{z} \cdot \vec{B}_o(t)), \quad (B.10)$$

where  $\vec{B}_o(t)$  is the magnetic flux density linking the loop and  $A_{eq}$  is the equivalent area of the sensor. In the frequency domain, this expression is

$$\begin{aligned} \tilde{V}_{oc}(\omega) &= j\omega \tilde{\Phi}(\omega) = A_{eq} j\omega \left( \hat{z} \cdot \tilde{\vec{B}}_o(\omega) \right) \\ &= A_{eq} j\omega \mu_0 \left( \hat{z} \cdot \tilde{\vec{H}}_o(\omega) \right). \end{aligned} \quad (B.11)$$

As noted in this expression, the magnetic field  $H$  and the magnetic flux density  $B$  are related by  $B = \mu_0 H$ , where  $\mu_0 = 4\pi \times 10^{-7}$  (H/m) is the permeability of free space.

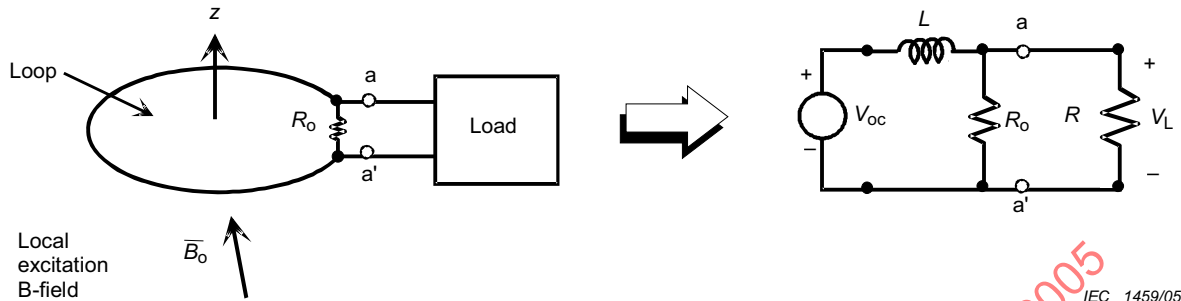


**Figure B.3 – Illustration of a simple B-field sensor, together with its Thevenin equivalent circuit**

Admitting the possibility of a shunt resistance  $R_o$  across the measurement loop, as seen in Figure B.3, the total load resistance applied to the loop is the parallel combination of this shunt and the resistance  $R$  representing the measurement chain. This total resistance is

$$R_t = \frac{RR_o}{R+R_o}, \quad (B.12)$$

and the measured voltage of this sensor then is given as

$$\begin{aligned} \tilde{V}_L(\omega) &= \frac{\tilde{V}_{oc}}{1+j\omega L/R_t} \\ &= \frac{j\omega A_{eq} \tilde{B}_{oz}(\omega)}{1+j\omega L/R_t} \\ &= \frac{A_{eq}}{\tau_{RL}} \tilde{F}(\omega \tau_{RL}) \tilde{B}_{oz}(\omega) \quad (\text{where } \tau_{RL} = L/R_t) \\ &\equiv \tilde{T}_{\text{sensor}}(f) \tilde{B}_{oz}(f) \end{aligned} \quad (B.13)$$

In equation (B.13) function  $\tilde{F}(\omega \tau_{RL})$  is again given by equation (B.4), but now with a time constant given as  $\tau_{RL} = L/R_t = L(R + R_o) / (RR_o)$ .

### B.2.1 Derivative (B-dot) sensors

For certain sensor parameters, the sensor response can be made to measure the rate of rise of the excitation B-field. For example, if  $1/\tau_{RL} = R_t/L >> 2\pi f_{\text{max}}$ , then the sensor response in the frequency domain is approximately

$$\tilde{V}_L(\omega) \approx j\omega A_{eq} \tilde{B}_{oz}(\omega) \quad (B.14)$$

and in the time domain, this expression is

$$V_L(t) \approx A_{eq} \frac{\partial}{\partial t} B_{oz}(t). \quad (B.15)$$

The requirement that  $R_t/L \gg 2\pi f_{max}$  can be met by removing the shunt resistance ( $R_o = \infty$ ).

As in the case of the E-field sensor, manufacturers usually describe these B-field sensors by the equivalent area  $A_{eq}$ , and the maximum bandwidth of operation  $f_{max} = R/(2\pi L)$ , under the assumption that the load resistance is a nominal 100  $\Omega$ .

### B.2.2 Direct H-field sensors

As in the case of the E-field sensors, by loading the sensing loop appropriately, it can be made to respond directly to the magnetic field. Specifically, if  $1/\tau_{RL} = R_t/L \ll 2\pi f_{min}$  where  $f_{min}$  is the minimum frequency of the spectrum to be measured, the load voltage becomes

$$\tilde{V}_L(\omega) = \frac{A_{eq}}{\tau_{RL}} \tilde{B}_{oz}(\omega) = \frac{A_{eq} \mu_0}{\tau_{RL}} \tilde{H}_{oz}(\omega). \quad (B.16)$$

Note that the requirement that  $(1/\tau_{RL})$  be small can be achieved by making the loop loading resistance  $R_o$  nearly a short circuit. However, in doing this, the measured voltage is reduced. Thus, there is a trade-off between the minimum cut-off frequency of this sensor and the voltage level provided to the measurement circuit.

### B.3 Electric field (or surface charge) ground plane sensors

It is also possible to develop EM field sensors that function properly when located near conductors. By assuming that the sensor will be located on an infinitely large, flat ground plane, image theory can be used to develop such sensors. For the case of measurements of the electric field, Figure B.4 shows the general configuration for an E-field sensor located over a conducting ground. This sensor is essentially one-half of the free-field sensor of Figure B.1, with the other half being the image in the ground plane.

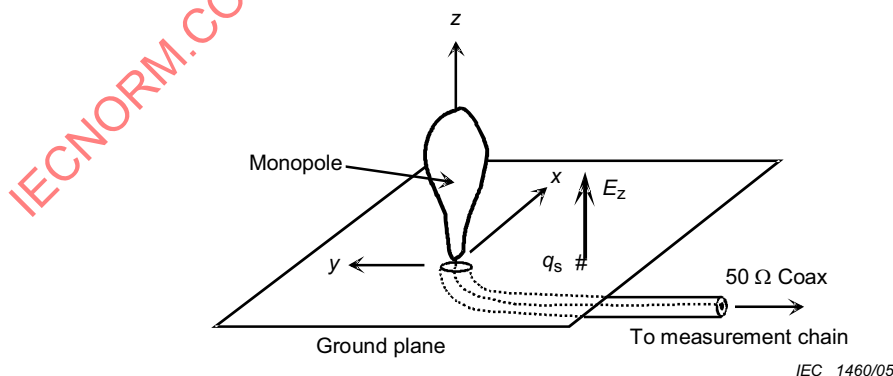


**Figure B.4 – Illustration of an E-field sensor over a ground plane used for measuring the vertical electric field, or equivalently, the surface charge density**

For the sensor of Figure B.4, the same equivalent circuit for the free-field sensor given in Figure B.1 is valid, with the exception that the equivalent area  $A_{eq}$  is one-half that of the free-field sensor, and the capacitance  $C$  is double. Moreover, the output from this type of sensor is unbalanced (coaxial), and is designed to operate into an impedance of  $50 \Omega$ , which corresponds to the measurement chain impedance level. Consequently, no balun is required for these types of sensors.

On the ground plane, the tangential E-field is zero (assuming a perfectly conducting ground plane) and the only component of the E-field is the vertical (z) component. This is the component of the E-field that excites the sensor.

**NOTE** Note that in this and all other EM field sensors discussed here, the sensor measures the *total* EM field, which is comprised of an incident field plus any reflected fields from nearby scattering bodies. In the case of sensors mounted on the ground plane, the scattered field is of the same order of magnitude as the incident field, and is such that the boundary conditions of tangential  $E = 0$  and normal  $H = 0$  on the ground plane are satisfied.

Typically, this sensor is operated as a D-dot sensor, with its voltage (across the  $50 \Omega$  load) being given by equations (B.7) and (B.8). In this instance, the internal sensor loading resistance  $R_o$  is zero, and this permits the sensor to measure the rate of rise of the E-field.

On a flat conductor, the electric flux  $D$  must terminate on an electrical charge density  $q_s$ . This is expressed as the boundary condition

$$D_{oz} = \epsilon_0 E_{oz} = q_s \quad (\text{coulombs/m}^2). \quad (\text{B.17})$$

This equation implies that the sensor in Figure B.4 is actually measuring the response to the local surface charge density. Thus, in the frequency domain equation (B.7) can be written in terms of  $q_s$  as

$$\tilde{V}_L(\omega) \approx -j\omega A_{eq} R \tilde{q}_s(\omega) \quad (R_o = 0; \omega \ll 1/RC) \quad (\text{B.18})$$

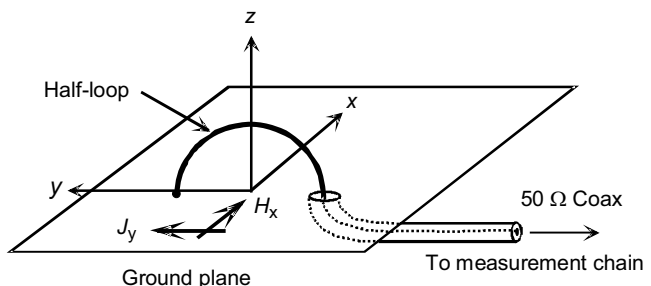
In the time domain, this expression for the load voltage is

$$V_L(t) \approx -A_{eq} R \frac{\partial}{\partial t} (q_s(t)) \quad (\text{B.19})$$

#### B.4 Magnetic field (or surface current) ground plane sensors

In an analogy with the imaged sensor for measuring E-fields on a ground plane, it is possible to have a half-loop structure to measure the magnetic field on the ground. This is illustrated in Figure B.5.

The electrical behaviour of this sensor is modelled by the Thevenin equivalent circuit of Figure B.3, and again by using image theory, we note that the equivalent area  $A_{eq}$  is one-half that of a full loop of the same dimension, the inductance  $L$  is one-half that of the full loop, and the output is an unbalanced coax feeding a  $50 \Omega$  load.



IEC 1461/05

**Figure B.5 – Illustration of the half-loop B-dot sensor used for measuring the tangential magnetic field, or equivalently, the surface current density**

This sensor is designed with the internal load resistance removed ( $R_o = \infty$ ), so that its response is proportional to the rate of rise of the field. The measured voltage across the 50- $\Omega$  load resistance is given by equations (B.14) and (B.15), with the sensor responding to the  $B_x$  (or  $H_x$ ) field component.

On the surface of the conducting ground plane the tangential H-field and surface current  $J_s$  are related by the boundary condition

$$\vec{J}_s = \hat{z} \times \vec{H}_{\tan} \quad (\text{A/m}). \quad (\text{B.20})$$

Consequently, for the sensor oriented to respond to the  $H_x$  field component, as shown in Figure B.5, it can be thought of as measuring the  $J_y$  component of the frequency domain surface current:

$$\tilde{V}_L(\omega) \approx j\omega A_{eq} \mu_0 \tilde{J}_y(\omega), \quad (\text{B.21})$$

and in the time domain, this expression is

$$V_L(t) \approx A_{eq} \mu_0 \frac{\partial}{\partial t} J_y(t). \quad (\text{B.22})$$

## B.5 Active sensors

An active sensor is one that contains internal electronics, which can perform a certain amount of signal processing of the measured signal. For example, such a sensor may contain an active integrator circuit that will eliminate the need for using an integrator in the measurement chain. In addition, such sensors can be designed to provide better noise characteristics, thereby increasing the sensitivity of the measurement chain.

Of course, like the fibre optic element in the measurement chain, an active sensor will require an external power supply, which will require periodic servicing in the field, and this can be inconvenient in some instances.

Active sensors are typically available from specialized vendors of EM field measurement equipment, and due to their relatively complex design, they are more expensive than the usual passive sensors. However, for special applications, they may be useful.

## B.6 Envelope detecting sensors

When measuring an amplitude modulated HPEM signal, often the only required information is the pulse shape and amplitude. In such cases, a slower digitiser and any associated fibre optic link can be used if the received signal is demodulated at the probe by a high-speed diode. This process leaves just the modulating signal to be recorded. The choice and calibration of the detector diode using the concepts of Clause 6 is critical and should be carefully considered. The diode is fitted after the balun. No integrator is required for such measurements.

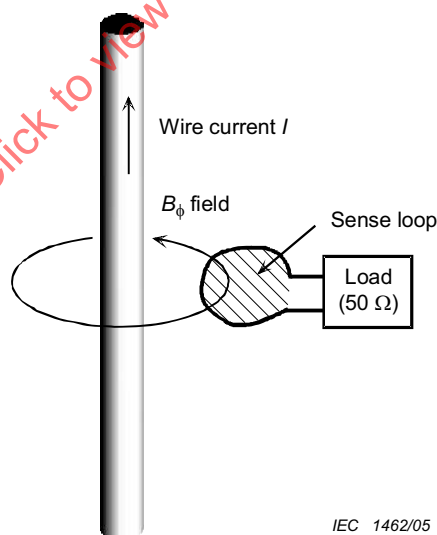
## B.7 Wire current sensors

Sensors can also be used to measure the current flowing in wires. This is done by measuring the local magnetic field surrounding the wire, and then relating it to the current in the wire. The basic concept of this type of sensor is shown in Figure B.6, and by a proper choice of parameters, it can be made to respond directly to the current instead of the rate of rise of the current.

In the frequency domain, the open circuit voltage induced in the sense loop is given by

$$\tilde{V}_{oc}(\omega) = j\omega \tilde{\Phi}(\omega) = j\omega M \tilde{I}(\omega), \quad (B.23)$$

where  $\tilde{I}(\omega)$  is the line current, and  $M$  is the mutual impedance between the line and the sense loop. For this sense loop, the equivalent Thevenin circuit of Figure B.3 can be used to determine the induced voltage across the load resistance. For this type of sensor, the output is generally an unbalanced 50- $\Omega$  load, so that a balun is not necessary.



IEC 1462/05

**Figure B.6 – Simplified concept for measuring wire currents**

### B.7.1 Self-integrating current sensor

The phrase “self integrating” is used to indicate that the measured waveform needs no further integration to reproduce the actual waveform of the stimulus. The actual construction of this current sensor is more complicated than that indicated in Figure B.6. Figure B.7 illustrates the important aspects of the sensor construction. First, to increase the sensor sensitivity, there can be multiple turns ( $N$ ) in the sense loop, and these loops are positioned around a magnetic material of high relative permeability,  $\mu$ , having an inner radius  $r_1$ , an outer radius  $r_2$  and

thickness  $w$ . This magnetic core serves to enhance the magnetic flux passing through the coils. In addition, a tuning resistance  $R_o$  is placed across the output of the sensor to adjust the lower frequency of the sensor bandwidth.

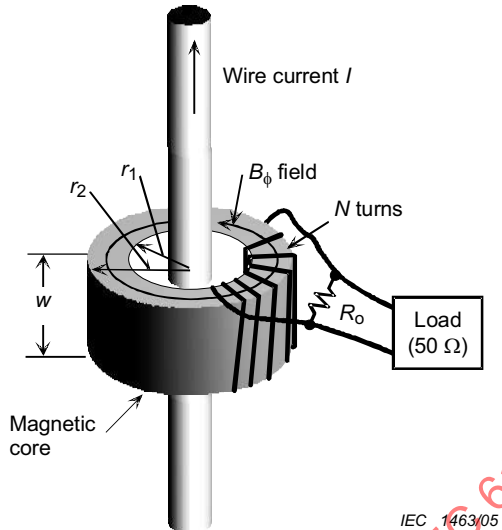


**Figure B.7 – Construction details of a current sensor**

For this sensor, the mutual inductance of the  $N$ -turn loop is given as

$$M = \frac{\mu \mu_0}{2\pi} N w \ln\left(\frac{r_2}{r_1}\right). \quad (\text{B.24})$$

The operation of this type of sensor is self-integrating. Using the equivalent circuit for the sensor given in Figure B.3, with the open circuit voltage given by equation (B.23), and assuming a low value for the tuning resistance  $R_o$ , the expression for the induced voltage in the  $50\text{-}\Omega$  load is

$$\begin{aligned} \tilde{V}_L(\omega) &= \frac{j\omega M \tilde{I}(\omega)}{1 + j\omega L/R_t} \\ &\approx \frac{M}{\tau_{RL}} \tilde{I}(\omega) \quad (\text{where } \tau_{RL} = L/R_t), \end{aligned} \quad (\text{B.25})$$

where  $\tau_{RL} = L/R_t$  is a time constant of the sense loop,  $L$  is the self inductance of the  $N$ -turn loop and  $R_t$  is the total parallel combination of  $R_o$  and the  $50\text{ }\Omega$  resistance,  $R$ , given by equation (B.12). Equation (B.25) is valid for frequencies larger than  $f_{\min}$  where the design requirement that  $1/\tau_{RL} = R_t/L \ll 2\pi f_{\min}$  must be observed. This latter requirement is done by making the shunt resistance  $R_o$  small.

Noting that the parameter  $M/\tau_{RL}$  in equation (B.25) has the dimensions of ohms, such sensors are usually characterised by this real-valued parameter, which is referred to as the “sensor impedance”,  $Z_p$ . In this way, the voltage induced across the  $50\text{-}\Omega$  resistance loading the sensor is given as

$$\tilde{V}_L(\omega) \approx Z_p \tilde{I}(\omega). \quad (\text{B.26})$$

This expression is valid as long as the operating frequency is greater than  $f_{\min}$ .

As an example of the measured current sensor impedance as a function of frequency, Figure B.8 presents the sensor impedance magnitude of a nominal 1- $\Omega$  current sensor over a frequency range from 1 000 Hz to 200 MHz. In this plot the differentiating nature of the sensor is evident for frequencies below about  $f_{\min} \approx 0,2$  MHz. Above this frequency, the response is reasonably flat with a sensor impedance of about 0,95  $\Omega$  – slightly below the specified 1- $\Omega$  value for the sensor.

It must be kept in mind that this sensor impedance is, in general, a complex valued function, and if the sensor is to be used at frequencies away from where equation (B.26) holds, the response must be evaluated using the more general complex equation in the first line of equation (B.25).

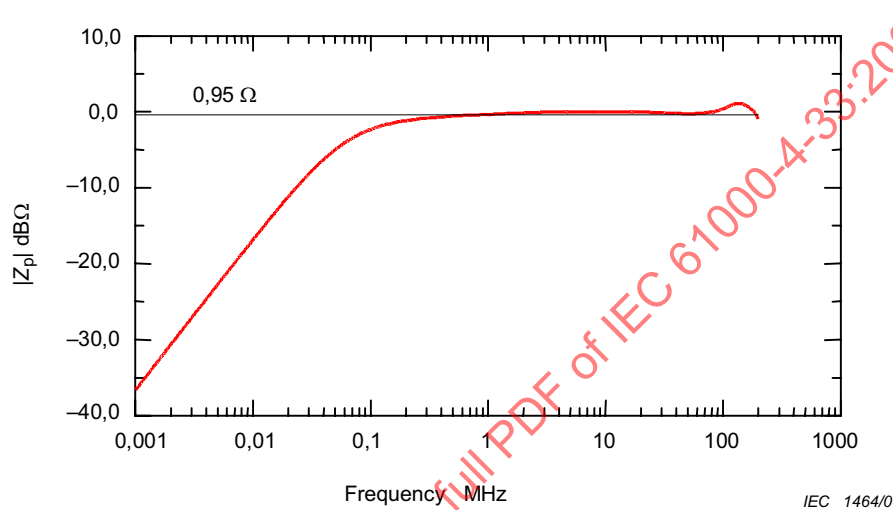


**Figure B.8 – Example of the measured sensor impedance magnitude of a nominal 1  $\Omega$  current sensor**

### B.7.2 In-line I-dot current sensor

An in-line current sensor is one that can be inserted into a tubular conductor to measure the external current. In this sensor, the output leads of the sensor are located inside the tubular conductor and run to the end of the conductor, thereby not interfering with the external current behaviour.

This sensor responds to the rate of rise of the current on the line, and has the geometry shown in Figure B.9. A circumferential cut is made in the outer circumference of the conductor, and this leads to an inner sensor chamber. The entire geometry is rotationally symmetric. This chamber serves as the “sense loop” for the B-field produced by the current flowing on the conductor.

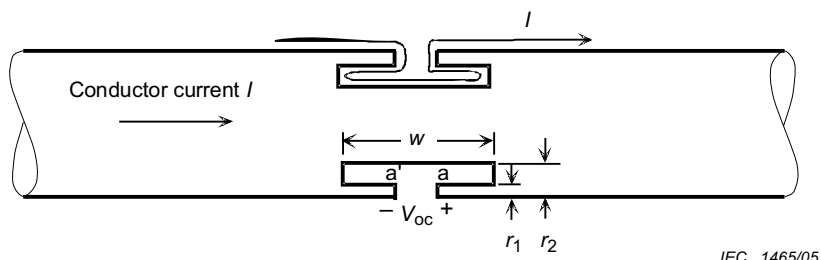


**Figure B.9 – Geometry of the in-line I-dot current sensor**